INTERNATIONAL JOURNAL OF AUTOMOTIVE AND MECHANICAL ENGINEERING
ISSN: 2229-8649 e-ISSN: 2180-1606
VOLUME 23, ISSUE 3, 2026, 13887 - 13907
DOI: https://doi.org/10.15282/ijame.23.3.2026.12.1048

RESEARCH ARTICLE

Prediction of tensile properties in fiber-reinforced composites by machine learning models

Md. Mominur Rahman[1, 2]*, Al Emran Ismail[3], Muhammad Faiz Ramli[3], Azrin Hani Abdul Rashid[1]

[1]Faculty of Engineering Technology, Universiti Tun Hussein Onn Malaysia, Johor, Malaysia
[2]Department of Textile Engineering, Faculty of Engineering, Daffodil International University, Dhaka, Bangladesh
[3]Faculty of Mechanical and Manufacturing Engineering, Universiti Tun Hussein Onn Malaysia, Johor, Malaysia

Abstract – The consistent design of fiber-reinforced composites (FRCs) remains difficult because of their heterogeneous structures and the complex relationships between processing parameters and material properties. Conventional tensile characterization is costly and destructive, while existing predictive models are often restricted to specific tensile parameters or single-fiber systems. This study addresses these gaps by developing machine learning (ML) models that simultaneously predict the tensile properties of pure and hybrid composites from experimental data. A total of 54 laminates were fabricated and tensile tested, comprising pure and hybrid combinations of carbon, Kevlar, and glass fibers in cross-ply and quasi-isotropic lay-ups with 4-, 8-, and 12-ply configurations. Several ML algorithms were implemented: baseline models (Linear Regression, K-Nearest Neighbor (KNN), Decision Tree, and Support Vector Machine), ensemble models (Random Forest, Gradient Boosting, Stochastic Gradient Boosting, Extreme Gradient Boosting, and Adaptive Boosting), and an artificial neural network (ANN). Experimentally, the Kevlar-glass bi-hybrid cross-ply 4-ply laminate (373.46 MPa) and the carbon-glass-Kevlar tri-hybrid cross-ply 8-ply laminate (389.79 MPa) outperformed the pure Kevlar laminate (326.40 MPa) in tensile strength. Among the models evaluated, KNN delivered the best predictive performance (R^2 = 0.87, MSE = 318.84, MAE = 7.73), followed by Stochastic Gradient Boosting (R^2 = 0.78), while the ANN showed only moderate accuracy (R^2 = 0.41). These findings confirm that ML, particularly instance-based and ensemble approaches, can predict the tensile behavior of fiber-reinforced composites from a limited experimental dataset. This reduces dependence on destructive testing and accelerates the design of high-performance hybrid composites for aerospace and automotive applications.

Article History
Received : 13 October 2025
Revised : 11 March 2026
Accepted : 21 May 2026
Published : 30 September 2026

Keywords
Fiber-reinforced composites
Tensile properties
Prediction
Machine learning

1. Introduction

Fiber-reinforced composites (FRCs) are widely used in the aerospace, automotive, marine, and sporting industries because of their high strength-to-weight ratio, corrosion resistance, design flexibility, low maintenance cost, fatigue resistance, and high specific strength and stiffness. Despite their increasing demand, the reliable design of FRCs remains a major challenge [1], as their mechanical properties are heavily influenced by numerous processing parameters with complex interactions, introducing significant uncertainties. Conventionally, these properties are characterized through destructive testing, which is expensive, time-consuming, and material-intensive [2]. Predictive modeling has emerged as a sustainable alternative to reduce the need for extensive experimentation. However, existing studies are limited and primarily focus on one or two tensile properties of single-fiber composite systems without considering hybrid fiber combinations. This limitation restricts the ability to predict the full range of tensile properties of both single- and hybrid-fiber composites. Therefore, there is a growing need for robust predictive models capable of accurately estimating multiple tensile properties using readily available input features. Among the available predictive techniques, machine learning (ML) has emerged as a state-of-the-art approach [3], offering design guidelines for optimization, reducing the design cycle, and compensating for limited experimental data by accurately predicting material properties.

Studies on unidirectional carbon fiber-reinforced polymers (CFRPs) have demonstrated that a Random Forest (RF) regressor trained on simulated microstructural data generated from representative volume elements (RVE) [4] achieved outstanding predictive accuracy (R^2 > 0.90) for the elastic modulus, shear modulus, ultimate strength, and impact toughness (R^2 = 0.98) with lower prediction errors [5]. Similarly, Decision Tree (DT) models have been applied to predict the elastic modulus and shear modulus of [0°/90°] carbon laminates. Although these models have demonstrated promising performance, they are limited by the exclusion of additional material and geometric design features [6]. Linear Regression (LR) models have also been developed using experimental data from polymer composites containing two or three filler types, achieving satisfactory predictive performance (R^2 ranged from 0.67 to 0.80) in predicting tensile strength, elongation, and wear resistance. However, these models lack robustness because they do not account for environmental factors, thus suggesting the need for validation under real-world conditions [7]. In addition, Gaussian Process Regression (GPR) has been employed to predict the open-hole tensile strength of composite laminates using simulation data based on the stacking sequence, ply orientation, and in-plane stiffness for laminate optimization [8].

Comparative studies involving multiple regression-based algorithms have demonstrated the superior performance of GPR over conventional models, including the Radial Basis Function (RBF), LR, Support Vector Regression (SVR), and several ensemble boosting techniques, in predicting the tensile strength and impact toughness of natural fiber

*CORRESPONDING AUTHOR | Md. Mominur Rahman | ✉ gn230006@student.uthm.edu.my
© 2026 The Authors. Published by Universiti Malaysia Pahang Al-Sultan Abdullah Press. This is an open access article under the CC BY-NC 4.0 license

composites. This superior performance was evidenced by the lower Root Mean Squared Error (RMSE) (99.13%) and Mean Absolute Error (MAE) (95.68%) values, indicating the potential applicability of GPR to other fiber-reinforced composite systems [9]. Concerning the composite system reinforced with treated jute fibers, XGBoost Regression exhibited better performance in tensile strength (R^2 = 0.9714) and hardness (R^2 = 0.9803) across several algorithms, such as AdaBoost, Extra Trees, Decision Tree, and Linear Regression. Moreover, the feature importance analysis identified the fiber content as the most influential input variable. Another study reported approximately 63% predictive accuracy for tensile-related properties (e.g., modulus, maximum stress, strain, and Shore hardness) across various regressors, such as DT, MLP, SVR, KNN, and LR [10]. These findings suggest that combining diverse regression algorithms can effectively capture the complex behavior of composite materials [11]. Similarly, blended regression models, especially with DT and RF, achieved a strong correlation (R^2 > 0.94) in predicting the elastic modulus of flex fiber composites. Although fiber orientation was identified as the dominant feature, the study considered only a limited number of variables and did not include the lay-up configuration or content as input parameters [12]. Similarly, GPR was reported to be the most reliable model compared to the Decision Tree, Support Vector Regression, and aggregated models for predicting the tensile strength of CFRPs, consistently achieving lower prediction errors [13].

Previous studies have shown that ANN models are effective in predicting mechanical properties, such as tensile and compressive strengths. A prior regression-based investigation reported that ANN models demonstrated superior performance in tensile (R^2 = 0.91) and compressive strength properties (R^2 = 0.88) [14]. In another study, the combined use of principal component analysis (PCA) and a genetic algorithm method was effective in improving a back-propagation neural network (BPNN) (R^2 > 0.89) when simulating the elastic, tensile, and compressive strengths of 2D microstructures of CFRP with micro-voids [15]. Another application involved the development of ANN models to predict the elasto-plastic stress response of short fiber composites with different fiber volume fractions, fiber orientations, and stress-strain states [16]. In high-performance concrete composites, ANN models have also been effective (R^2 > 0.90) for predicting the tensile strength and tensile strain based on the design characteristics and strain rates of concrete [17]. Likewise, some models using ANN demonstrated high accuracy (R^2 > 90%) in predicting the stress-strain performance of natural and hybrid composites (e.g., banana-HDPE and plantain fiber-carbon nanotube); however, their generalizability was limited owing to the exclusion of important design parameters [18]-[19]. For natural fibers, the physical properties of cellulose and moisture content were used as input variables for a dual ANN structure consisting of the BPNN structure and the SNN architecture [20], which achieved more than 95% accuracy in predicting Young's modulus (YM), Universal Tensile Strength (UTS), and elongation at break. In contrast, convolutional neural networks (CNN) have been effectively used to predict the mechanical response based on direct prediction from microstructural images. One study utilized a CNN to accurately predict the stress distribution outlines in E-glass composites with localized stress concentrations in the fiber regions [21]. Deep Neural Networks (DNNs) have also been used to predict the apparent strength using microscopy images in both experimental and simulated data, which improved the computational speed and accuracy; nevertheless, further research is required to include the effects of fiber arrangement and density [22]. Moreover, a CNN combined with PCA successfully predicted tensile stress and strain properties based on a simulation of the structural input characteristics, with maximum errors of 2.5% for the tensile strength and 10% for the elastic modulus. DenseNet121 is also superior to other CNN models in this field [23]. When coupled with a DNN, transfer learning (TL) outperformed DNN models in predicting the elasto-plastic behavior using combined experimental and simulated stress-strain data, especially for different reinforcement volume fractions and shapes [24].

Hybrid modeling approaches have received considerable attention to improve the predictive accuracy, robustness, and applicability of FRCs' mechanical behaviors by combining ANN and Support Vector Machine (SVM) models with mixed literature data. Despite obtaining good results, variations in manufacturing conditions and composite types from various datasets were deemed to affect the generalizability of the models [25]. In comparison, high-performance fiber-reinforced cementitious composites (HPFRCC) obtained the best results for the compressive strength prediction by XGBoost in training (R^2 = 0.993) and testing (R^2 = 0.957) [26]. Similarly, various machine learning models, including ANN, SVR, RF, GBM, CNN, and RNN, have combined data from literature and open-source datasets to predict the tensile strength of CFRPs. In a classification algorithm, a top-down trainable wavelet transform with the fiber volume fraction and medium density was identified as the most important input variable for the best model [27]. In another study, ANN and GPR models attained good outcomes in predicting the tensile and flexural properties of triaxial-braided composites made from graphene nanoplatelets [28]. Similarly, ANN and other regressors on hybrid glass-carbon composites reported the best results in predicting tensile strength, indicating the general effectiveness of ANN for the prediction of other mechanical properties [29]. Although significant predictive progress has been made in the field of machine learning, there remains a gap in end-to-end models that can reliably predict the complete set of tensile properties of pure and hybrid fiber-reinforced composites. Furthermore, previous research has mainly focused on simulations, existing literature, open-source datasets, single-fiber systems, simple sets of mixtures, and simple modeling. This study aims to address these limitations by testing several baseline machine learning models LR, SVM, DT, KNN; ensemble learning models like RF, AdaBoost (Adaptive Boosting), Stochastic Gradient Boosting (SGB), Extreme Gradient Boosting (XGBoost), and Gradient Boosting (GB); and a neural-based model and ANN to predict tensile properties. This was achieved by analyzing experimental data for a wide range of laminates with varying stacking sequences, number of plies, and pure and hybrid (mixed carbon/Kevlar/glass reinforced epoxy) with different fiber compositions, followed by an analysis of the input features that dominate the tensile properties of glass-reinforced epoxy.

2. Methods and Materials

2.1 Composite Fabrication

The specifications of the three types of woven fabrics used in this study are presented in Table 1. The specimens were fabricated using an epoxy resin and hardener with an epoxy-to-hardener ratio of to 1:2. An equal amount of resin was applied to each layer of the fabric. Rectangular composite plates were manufactured in three groups, each consisting of six plates (three quasi-isotropic laminates and three cross-ply laminates with 4-, 8-, and 12-ply configurations). The first group consisted of pure (single-constituent) composites made entirely of carbon, Kevlar, or glass fibers. The second group contained hybrid two-constituent composites made of carbon (50%) and Kevlar (50%), carbon (50%) and glass (50%), and Kevlar (50%) and glass (50%). The third group consisted of three-constituent hybrid composites with 50%-25%-25% fiber compositions: Kevlar (50%), carbon (25%), and glass (25%); carbon (50%), glass (25%), and Kevlar (25%); and glass (50%), carbon (25%), and Kevlar (25%).

Table 1. Technical details of carbon, Kevlar, and glass fabric

Items	Carbon	Kevlar	Glass
Fiber Orientation	0º, 90º	0º, 90º	0º, 90º
Color	Black	Yellow	White
Weave	2 × 2 Twill	2 × 2 Twill	1 × 1 Plain
Format	Woven	Woven	Woven
Weight (GSM)	200	300	600
Fiber Type	Carbon	Kevlar	E-Glass
Ends (cm)	5	4.75	-
Picks (cm)	5	4.75	-
Tensile Strength (MPa)	3758	3000	-
Tensile Modulus (GPa)	231	112.4	-
Density (g/cm^3)	1.8	1.44	2.55
Consolidated Thickness (mm)	0.28	0.40	0.52

Two distinct lay-up orientations were used in this study: cross-ply and quasi-isotropic lay-ups. The composition codes of the fabricated laminates are listed in Table 2. For the fabrication of the laminates, Kevlar was used as the outermost layer because of its excellent impact resistance and energy absorption, whereas carbon and glass fibers were used as the remaining reinforcement layers. Resin saturation was carried out using the manual wet lay-up technique followed by vacuum bagging, and the selected steps are shown in Figure 1. Reinforcement fabrics measuring 325 mm × 325 mm were carefully cut to size using a paper template to maintain fiber orientations of 0°, 90°, 45°, and −45°. The laminates were fabricated by sequentially stacking the cut fabrics inside a vacuum bag, with each layer impregnated using the epoxy-hardener mixture within its 22-minute pot life. The laminates were cured at ambient temperature for 24h before demolding.

Table 2. Coding details of fabricated laminates

Layer Composition (%)	Symmetric Layer Order	Code Letter	Ply Type	No. of Ply	Coding Example (C=Carbon, K=Kevlar, G=Glass)
100%	[C/C/C/C]s, [K/K/K/K]s [G/G/G/G]s	C, K, G	1= Cross ply= [0°/90°/90°/0°]s, 2 = Quasi-isotropic= [45°/0°/-45°/90°]s	4, 8, 12	C 1 - 4 → Ply Type (1/2); → No. of Ply (4/8/12); → Composition 1 (100%)
50%-50%	[K/C/C/K]s, [C/G/G/C]s, [K/G/G/K]s	CK, CG, KG	1= Cross-ply= [0°/90°/90°/0°]s, 2 = Quasi-isotropic= [45°/0°/-45°/90°]s	4, 8, 12	CG 2 - 8 → Ply Type (1/2); → No. of Ply (4/8/12); → Composition 2 (50%); → Composition 1 (50%)
50%-25%-25%	[K/C/G/C]s, [K/G/C/K]s, [K/G/G/C]s	CGK, KCG, GCK	1= Cross ply= [0°/90°/90°/0°]s, 2 = Quasi-isotropic= [45°/0°/-45°/90°]s	4, 8, 12	GCK 1 - 12 → Ply Type (1/2); → No. of Ply (4/8/12); → Composition 3 (25%); → Composition 2 (25%); → Composition 1 (50%)

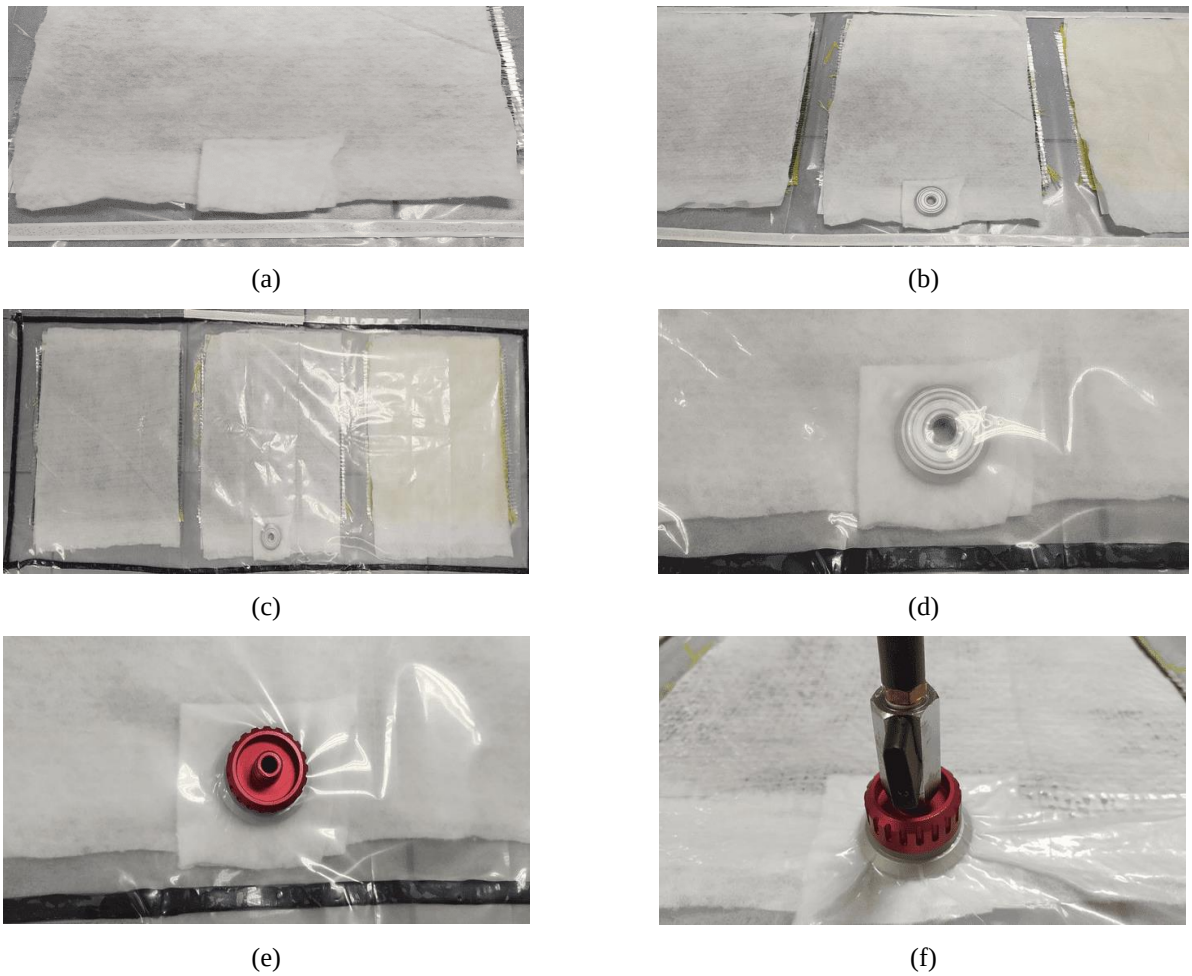


Figure 1. Manual wet lap of vacuum bagging technique: (a) Bleeder fabric double layering; (b) Vacuum connector (1st part) setting; (c) Polythene sheet (top) layering and sealant tape closing; (d) Hole making above 1st part of vacuum connector for air exhaustion; (e) Vacuum connector (2nd part) setting; (f) Vacuum connector (2nd part) and air exhaust pipe connecting

2.2 Tensile Testing

The composite specimens were tested in tensile according to the details in Table 3.

Table 3. Tensile strength test details

Items	Test Information
Standard	ASTM D3039/D3039M
Instrument Name	Universal Testing Machine
Capacity	50 kN
Sample Length	250 mm
Sample Width	25 mm
Cross Head Speed	2 mm/min
Test Type	Constant Strain Rate
Acquisition of Raw Data	Time, Load, Elongation

2.3 Machine Learning Modeling

This study incorporated 12 input features (cloth weight, consolidated thickness per ply, computed thickness, actual thickness, specimen length, width, area, layer composition, lay-up orientations, lay-up type, and number of plies) to predict the corresponding output variables in terms of the maximum load (kN), maximum elongation (mm), maximum strain (%), elastic modulus (GPa), breaking stress (MPa), and tensile strength (MPa). Using these features and output variables, machine learning methods were used to predict the tensile properties of composite laminate materials developed from carbon, Kevlar, glass fiber, and combinations of these fiber materials. Several baseline models were used, including LR, KNN, SVM with a linear kernel and a RBF kernel, and DT. The ensemble methods included RF, AdaBoost, GB, SGB, and XGBoost. The neural model used was an ANN with a single hidden layer. The overall machine learning pipeline entailed the processes of feature identification, data preparation and preprocessing,

exploratory data analysis (EDA), feature selection, and data augmentation, which generated 648 samples that were split into 80% training and 20% testing sets. Additionally, five-fold cross-validation was performed, followed by a performance evaluation.

2.3.1 Fundamental models

Fundamental models such as KNN and SVM offer simplicity and interpretability, with SVM handling nonlinear relationships through kernel functions. DT models provide interpretable predictions but may be prone to overfitting, whereas LR models capture linear relationships. Linear Regression models the relationship between the input features and the target variable using Eq. (1), where the slope is m and the intercept is *c*.

$$y = mx + c \tag{1}$$

KNN is an instance-based model, which is expressed as Eq. (2). It calculates Euclidean distances as $\mathrm{d}(\mathbf{x}, \mathbf{x}_\mathrm{i})$ and selects the k nearest distances where x =Input features; $N_k(x)$= set of k adjacent neighbors in data; y_i: Output of the ith neighbor; k = User fixed neighbors' number.

$$\hat{y}(x) = \frac{1}{k}\sum_{i \in N_k(x)} y_i \tag{2}$$

In contrast, SVM models with linear and RBF kernels were used to model nonlinear relationships, which are presented in Eq. (3). A decision function f(x) is built where $\phi(x_i)$ represents a function, while w and b are weight and bias constants, respectively [30].

$$f(x) = \prec w, \phi(x_i) \succ + b \tag{3}$$

$$f(x) = \sum_{i=1}^{n} (\hat{}ai - ai))\kappa(x, xi) + b \tag{4}$$

Otherwise, DT is applied for interpretable mapping of features (see Eq. (5)), where x_1, x_2, x_3..., x_k are the predictors and Y is the target [31].

$$(X, y) = (x_1, x_2, x_3, \ldots, x_k, Y) \tag{5}$$

2.3.2 Ensemble models

Numerous ensemble methods can be employed to address overfitting. These methods improve prediction accuracy by combining several models by combining multiple models to improve prediction performance for high-dimensional data. For instance, RF groups multiple decision trees to improve accuracy and robustness (see Eq. (6)), while AdaBoost, SGB, GB, and XGBoost models continuously correct prediction errors [32].

$$\hat{y}(x) = \frac{1}{T}\sum_{t=1}^{T} \hat{y}_t\,(x) \tag{6}$$

where $\hat{y}_\mathrm{t}(\mathrm{x})$is the prediction of decision tree while T is the number of trees.
AdaBoost is another ensemble approach, which can be operated using Eq. (7) [32].

$$H(x) = \sum_{t=1}^{T} \alpha_t\, h_t(x) \tag{7}$$

where x =Input; $h_t(x)$ is the prediction of weak learner; α_t is the weight of the tth learner, and T: Total number of weak learners.
On the other hand, GB functions on the entire set of data quickly without performing the subsampling process, whereas SGB operates casually by subset samples. The final prediction, $F_M(x)$, is an additive model of the M decision tree in Equation (8), where: F_0 = Initial prediction (mean/median of the target); α = Learning rate, and $h_m(x)$ = Prediction of the m^{th} tree. It is worthy to note that both approaches work using a similar equation but with a dissimilarity in updating w and b per sample (or mini-batch) rather than the full data [33].

$$F_M(x) = F_0 + \alpha \sum_{m=1}^{M} h_m\,(x) \tag{8}$$

Another ensemble tree is the Extreme Gradient Boosting (XGBoost) model. It functions according to the boosting principle, which is different from the random forest (RF) as it works by training trees successively.

2.3.3 Neural network model

An Artificial Neural Network (ANN) captures nonlinear and complex interactions, which function according to Eq. (9). The first and second hidden layers consisted of 128 and 64 neurons, respectively, whereas the output was 1. The ReLU and sigmoid activation functions, together with the Adam optimizer, were used to balance fitting issues. Furthermore, the number of epochs, batch size, and learning rate were 100, 16, and 0.001, respectively. This can be achieved using Eq. (10), where w_{ij} is the weight function, x_i is the summing inputs, and b_i is the bias for obtaining y_i [34].

$$y_i = \sum_{i=1}^{n} w_{ij} x_i + b_i \tag{9}$$

The output, z_I, is obtained by using the activation f function on y_i, as is shown in Eq. (10).

$$z_i = f(y_i) \tag{10}$$

2.3.4 Models' validation and performance evaluation

The machine learning models underwent k-fold (k = 5) cross-validation. This was done by randomly splitting the data into five sets, with each dataset used for testing once, while the remaining four datasets were used for training. This process was repeated for each fold to calculate the mean performance metrics. A similar process was repeated for all five data folds, where each data point was used for both validation and training. Three metrics were used to measure the accuracy of the models: Mean Squared Error (MSE), Mean Absolute Error, and R-squared (R^2), as illustrated by Equations (11), (12), and (13), respectively.

$$MSE = \frac{1}{n}\sum_{i=1}^{n}(y_i - \hat{y_i})^2 \tag{11}$$

where y_i is the real value, $\hat{y}_i$ is the predicted value of prediction, and n is the number of samples.

$$MAE = \frac{1}{n}\sum_{i=1}^{n}/y_i - \hat{y_i}/ \tag{12}$$

$$R^2 = 1 - \frac{\sum_{i=1}^{n}(y_i - \hat{y}_i)^2}{\sum_{i=1}^{n}(y_i - \bar{y})^2} \tag{13}$$

where $\bar{y}$ is the average of the real value and R^2 measures the amount of variance, and a value close to 1 represents a good fit.

3. Results and Discussions

3.1 Stress-Strain Analysis

Based on the analysis of the tensile stress–strain curves shown in Figure 2, the mechanical behavior of the fiber-reinforced epoxy composites provides important information regarding the influence of the fiber constituents and hybridization. For the 100% composites, carbon (C) exhibited the sharpest initial slope, indicating high stiffness, but frequently failed in a brittle manner with little plastic deformation. Kevlar (K) exhibits distinctive properties of high strength and significant ductility, with a pronounced yield point and high strain-to-failure, indicating superior energy absorption and toughness. Glass (G) provided a balance between moderate strength and good ductility, and it exhibited a more gradual failure than carbon. For the 50%/50% composites, Kevlar-Glass (KG) was an exception, where the tensile strength exceeded that of the individual constituents. The curve displayed a pronounced strain-hardening zone, practically uniting the toughness of Kevlar with the load-bearing capability of glass. The carbon-glass (CG) hybrid was stiffer, and while its linear response offered the benefit of carbon's rigidity, it exhibited a lower strain capacity. The carbon-Kevlar (CK) hybrid exhibited intermediate behavior, providing a balance between stiffness and ductility. Unlike the tri-constituent composites (50%/25%/25%), the carbon-dominated CGK composite exhibited the highest tensile strength among all groups (extremely steep elastic region); however, this might be at the expense of ductility. The hybrid produced under Kevlar domination (KCG) displayed remarkable damage tolerance while retaining its strength but with a considerably larger strain-to-failure. The glass-dominated (GCK) hybrid might have a lower stiffness but exhibits greater ductility, resulting in a more graceful failure pattern. In this case, the shape of the curves was a direct indicator of the failure mode. Carbon-rich composites displayed sharp drop-offs post-peak stress, whereas Kevlar-rich composites showed a more gradual failure response with a long period of reasonably steady stress until fiber pull-out and matrix cracking occurred.

For 100% composites, Figure 2 (a) shows the tensile behavior of the pure composites. The carbon composite exhibited the best characteristics in the quasi-isotropic C2-8 configuration (290.04 MPa strength, 13.66 GPa modulus), although the cross-ply strength decreased as the number of plies increased [35]. Kevlar exhibited superior energy absorption, with the cross-ply K1-4 possessing the maximum strength (326.40 MPa) and modulus (13.68 GPa), although the quasi-isotropic variants had a 30-31% reduction in the property due to the off-axis sensitivity [36]. The glass fiber composite exhibited a strong dependence on fiber orientation, and the cross-ply G1-04 exhibited the maximum strength value (303.64 MPa), whereas the quasi-isotropic samples exhibited higher strain capacity but considerably lower stiffness [36] [37]. Figure 2 (b) demonstrates the synergistic effects of hybridization for the 50% + 50% composites. Carbon-Kevlar (CK) exhibited a balanced performance in cross-ply CK1-8 (221.93 MPa tensile strength and 13.15 GPa modulus), although the quasi-isotropic configuration exhibited a reduced performance [38]. The carbon-glass (CG) hybrid had improved performance in CG1-4 (251.64 MPa strength, 14.94 GPa modulus), with retained strength in thicker laminates [38]. Importantly, Kevlar-glass (KG) hybrids exhibited superior performance compared to their constituent materials in KG1-04 (373.46 MPa strength), but exhibited a unique thickness-dependent behavior with a higher absolute load capacity [38]. Figure 2 (c) shows the advanced property combinations for the 50% + 25% + 25% composites. The deformation and stress-strain analysis of their performance with CGK1-08 revealed exceptional strength (389.79 MPa) with maintained stiffness, albeit below the simulated benchmark. The Kevlar-dominated (KCG) hybrids possessed excellent damage tolerance levels, with KCG1-12 retaining 97.2% of the 4-ply strength with a 6.25% strain [39]. The glass-dominated (GCK) composites demonstrated anomalous inverse values of the stiffness-strength relationship in GCK1-08 (256.00 MPa strength but 49.3% reduced stiffness), implying thickness-dependent failure mechanisms [39]. Notably, quasi-isotropic versions consistently underperformed across all ternary systems, underscoring the important role of fiber alignment for complex hybrids.

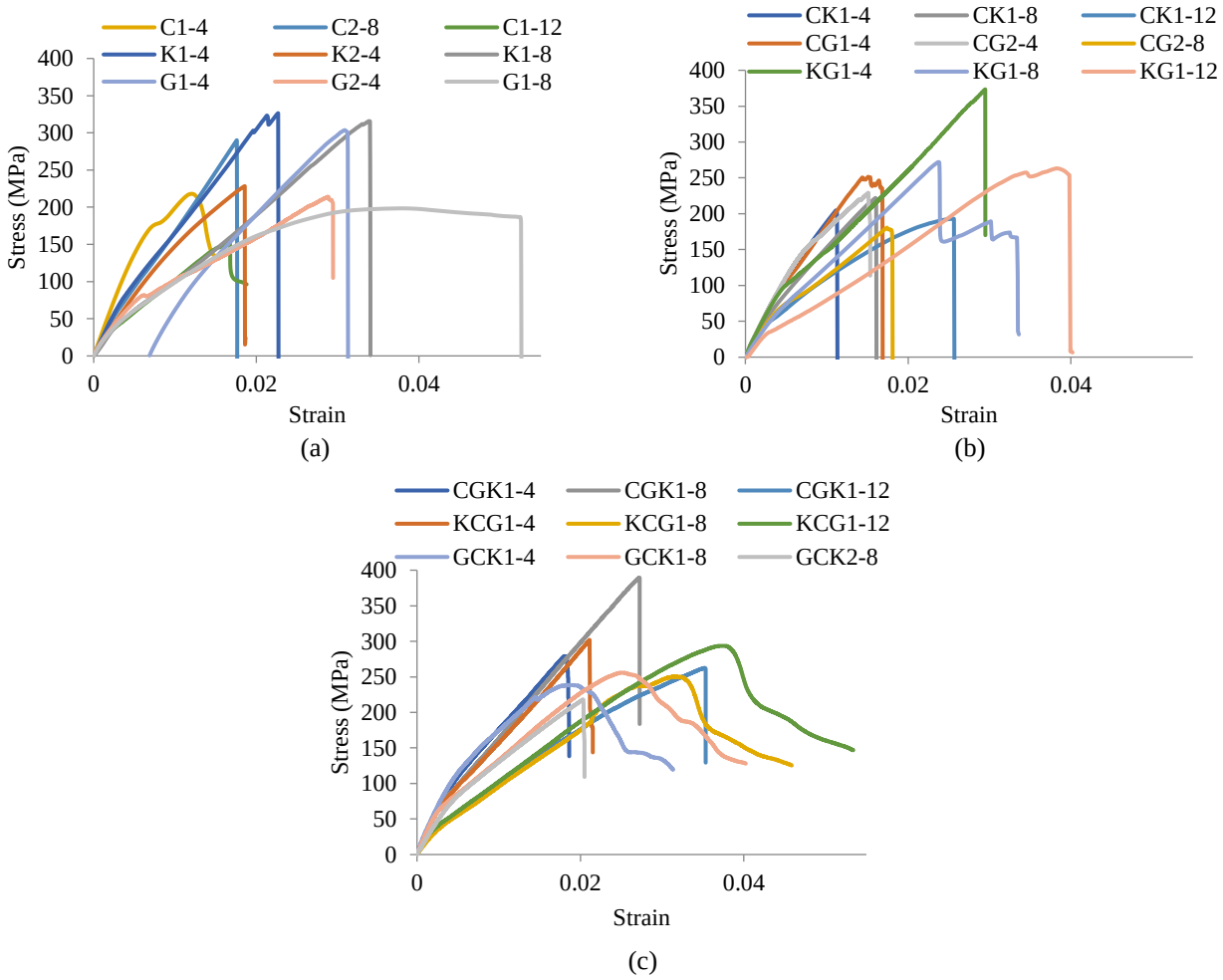


Figure 2. Stress versus Strain curves: (a) for 100%; (b) for 50% + 50%; and (c) for 50% + 25% + 25% compositions

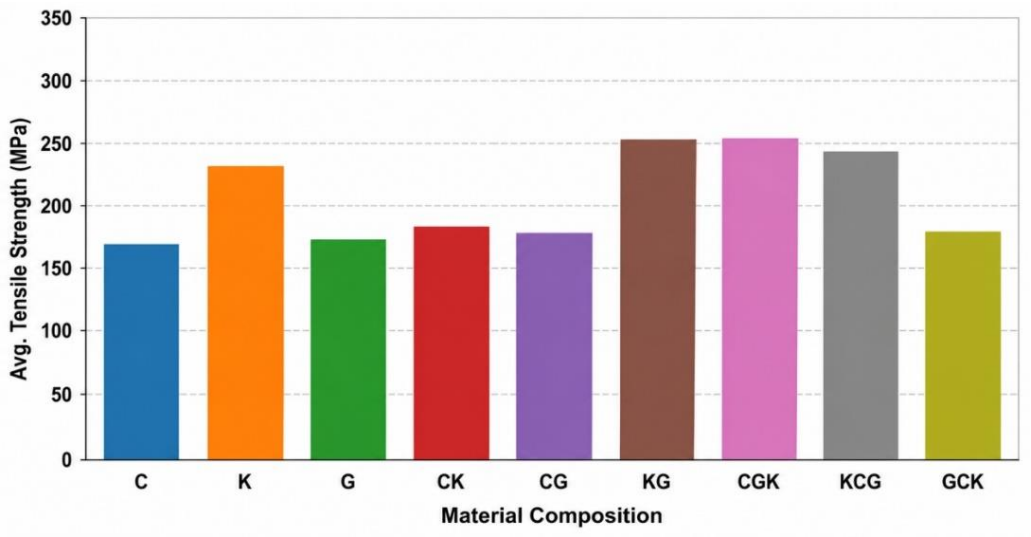


Figure 3. Material compositional effects on average tensile strength

3.2 Materials Composition Effects on Tensile Strength

Figure 3 shows the tensile strength of the different material compositions, demonstrating that the various fiber Figure 3 shows the tensile strength of the different material compositions, demonstrating that the various fiber compositions exhibit different performance trends. 100% Kevlar (K) had the highest tensile strength (K1-4, 326.4 MPa), which also exceeded the tensile strength of a bi-directional plain woven Kevlar-49 fabric epoxy composite of 6 plies [40] due to its inherent toughness and energy absorption. The results align with the two-layer cross-ply Kevlar (1.36 mm) and glass (2.14 mm) composites with tensile properties of Kevlar composites [41], as well as 3D woven glass/polyester fire-retardant sandwich composite [42]. On the other hand, 100% Carbon (C) and 100% Glass (G) exhibited moderate

strength, with the former surpassing the latter due to its better stiffness (e.g., C1-4: 218 MPa vs. G1-4: 303.6 MPa). Among the hybrids, 50% Kevlar + 50% Glass (KG) was distinguished (KG1-4: 373.48 MPa) and benefited from the ductility of Kevlar and the stiffness of glass. Among the ternary hybrids, the carbon-dominated CGK composite exhibited the highest tensile strength (CGK1-8: 389.76 MPa), whereas the glass-dominated GCK composite showed the lowest performance (GCK1-12: 95.45 MPa), probably due to resin dominance in thicker laminates. Overall, Kevlar-rich hybrids (KG, KCG) and carbon-dominated ternary mixes (CGK) offer the best applications for strength.

3.3 Fiber Orientation Effects on Tensile Strength

The comparison of fiber configurations in Figure 4 demonstrates the superior tensile performance of cross-ply configurations compared with quasi-isotropic designs. The results show that the cross-ply K1-4 (100% Kevlar) laminate achieved 326.4 MPa, whereas the quasi-isotropic K2-4 laminate achieved 228.3 MPa. Similarly, the cross-ply C1-4 laminate achieved 218 MPa compared with 143.5 MPa for the quasi-isotropic C2-4 laminate. A similar trend was also observed in the bi- and tri-hybrids (e.g., CK1-4: 204.6 MPa vs. CK2-4: 149.6 MPa), as cross-ply configurations are expected to provide better resistance to uniaxial loading, which is in agreement with [43]. Cross-ply lay-up is preferred for applications that require tensile loads, although quasi-isotropic designs may be suitable where multi-axial loading is required. Overall, material composition and lay-up design have an interdependent effect on tensile strength. The results emerged from the feature importance analysis, which clearly showed that fiber content was the most important factor in determining the tensile strength of composite laminates [10]. Similarly, fiber orientation and direction were also reported as dominant features influencing tensile behavior in other studies [12].

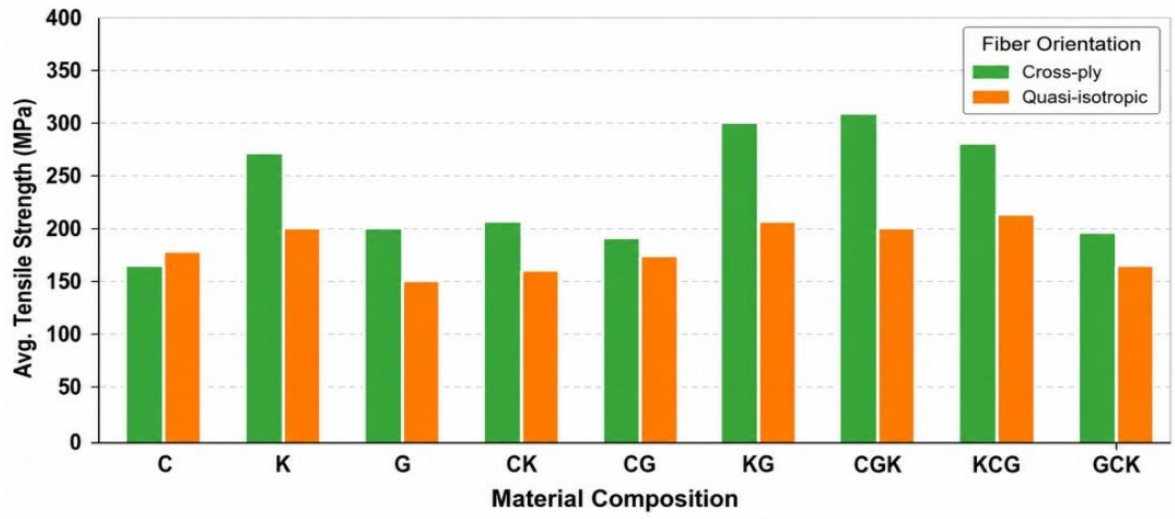


Figure 4. Fiber orientation effects on average tensile strength

3.4 Number of Plies Effects on Tensile Strength

The tensile test results in Figure 5 reveal a complex relationship between tensile strength and the number of plies for different fiber-reinforced epoxy composites. For 100% carbon (C) samples, tensile strength reduced as the ply count increased, suggesting possible limitations in load distribution or the presence of interfacial defects in thicker laminates. The findings resonate with prior tensile property research, which reported that 1-mm carbon composite had 0^o, 45^o, and 90^o fiber orientations [35]. Conversely, 100% Kevlar (K) composites showed mixed trends, with 8-ply composites (e.g., K1-8: 315.8 MPa) being superior to 4-ply and 12-ply samples, possibly due to improved fiber alignment and stress transfer. The findings are consistent with the reported modulus of elasticity of a 3.4-mm 2D plain-woven Kevlar-reinforced polyester composite, ranging from 1.3045 to 4.4247 GPa [37]. The 100% glass (G) samples showed a decreasing trend in strength. For hybrid composites (50% + 50%), the carbon-Kevlar (CK) series had superior performance (221.9 MPa, 8-ply configurations) in terms of the trade-off between strength and stiffness. However, the carbon-glass (CG) hybrids exhibited the maximum stress at 4 plies (CG1-4: 251.5 MPa) with brittleness issues at higher ply count. The Kevlar-glass (KG) hybrids exhibited superior strength for 12-ply samples (KG1-12: 263.2 MPa) and combined the ductility of Kevlar fiber and the stiffness of glass fiber. Overall, the tensile properties of bi-fiber reinforced composites align with the evaluation of tensile properties of a 5-ply bi-fiber reinforced composite having carbon, Kevlar, and glass of different stacking sequences. Meanwhile, Carbon-Kevlar-Carbon-Kevlar-Carbon had the highest tensile strength of 385.09 MPa, with CK having 357.33 MPa, GK having 234.07 MPa, and KG having 361.71 MPa [44]. In trihybrids (50% + 25% + 25%), the CGK (50% carbon) series attained a higher strength value of 389.76 MPa (for CGK1-8), revealing synergistic reinforcement. Both KCG (50% Kevlar) and GCK (50% glass) hybrids showed medium performance, with KCG1-12 recording 293.71 MPa, indicating Kevlar's contribution to toughness. Overall, the optimal ply count depends on fiber type and hybridization, indicating that increasing the number of plies does not necessarily improve tensile strength across different stacking sequences [45].

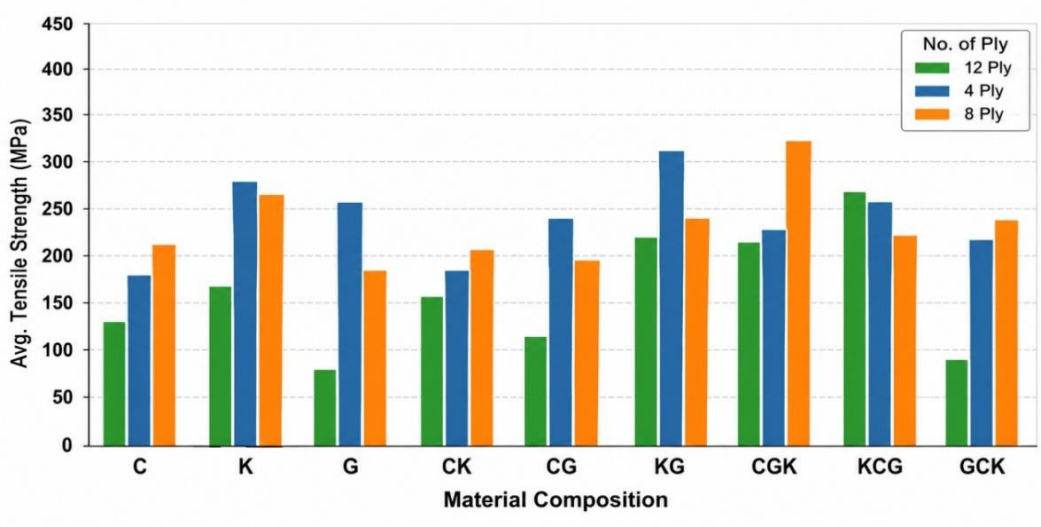


Figure 5. The effect of the number of plies on the average tensile strength

3.5 Machine Learning Models' Predictive Analysis

The discussion of findings is based on the predicted results of three supervised models, five baseline models, five ensemble models, and one neural network model.

3.5.1 Dataset preparation with feature identification

The selection of features for input has an influence on the predictive accuracy, generalizability, and interpretability of fabricated composites for tensile properties. The primary dataset consisted of 162 data points (from three tests for each of 18: 100%-50%, and 50%-25%-25%), with 54 data points generated (18 for each of the three types).

3.5.2 Pre-processing

The pre-processing phase included an in-depth inspection and cleaning of the dataset to prepare it for analysis. The dataset was found to contain 11 floating-point and 8 integer variables with two null values in the Modulus and Breaking Stress variables. A built-in function was used to indicate the missing (null) values. Two categorical variables of sample ID were excluded because they were irrelevant to the analysis and were used only for identification. This was followed by exploratory data analysis (EDA), as shown in Table 4. The close match between calculated and actual thickness (mm) metrics recorded a median value of 3.20 mm and 3.45 mm, respectively, thus supporting the validity of thickness calculations. The Mechanical Performance Combination showed significant variability in Maximum Load (kN), Tensile Strength (MPa), Modulus (GPa), Maximum Elongation (mm), Max Strain (%), and Breaking Stress (MPa). The data distribution patterns in Figure 6 show that the Max Load (kN) and Tensile Strength (MPa) distributions had rightward skewness due to outliers but approached near symmetry. In contrast, Modulus (GPa) has a wide multimodal distribution. Deformation metrics had different behaviors: Max Elongation (mm) was right skewed, while Max Strain (%) was well clustered with slender tails. Breaking Stress (MPa) also had a bimodal distribution.

Table 4. Statistical EDA of tensile properties

Parameters	Max Load (kN)	Max Elongation (mm)	Modulus (GPa)	Max Strain (%)	Breaking Stress (MPa)	Tensile Strength (MPa)
Count	162	162	162	162	162	162
Mean	16.24	6.02	8.43	4	130.49	203.85
STD	7.76	3.06	3.91	2.03	76.41	81.1
Min	3.65	1.19	0.22	0.8	2.32	38.42
25%	10.23	4.35	5.27	2.9	73.32	153.86
50%	14.74	5.52	7.81	3.68	118.94	205.14
75%	20.13	7.03	10.88	4.68	176.18	258.36
Max	38.59	23.63	24.27	15.75	409	413.38
Uniqueness	158	148	158	139	159	161

Figure 7 shows the case of outliers. For Maximum Elongation (mm), extreme values reached 15 mm and were far above the upper quartile, indicating the presence of unusually ductile specimens. Max Load (kN) had an outlier greater than 30 kN, suggesting that some samples had an extraordinary load-bearing capacity. Tensile Strength (MPa) recorded outliers around 400 MPa, indicating high-performance specimens or measurement artifacts. Breaking Stress (MPa) was also evident in the extreme values near 400 MPa, reinforcing the previously observed bimodal distribution. Modulus (GPa) showed outliers beyond 20 GPa, which might be related to material inconsistencies or testing irregularities. The Maximum Strain (%) boxplots revealed closely scattered data and several outliers, indicating similar deformation

behavior in most samples. These outliers were handled using the standard scaling method by including the values within the 0-to-1 range to ensure proper prediction modeling, as shown in Figure 8.

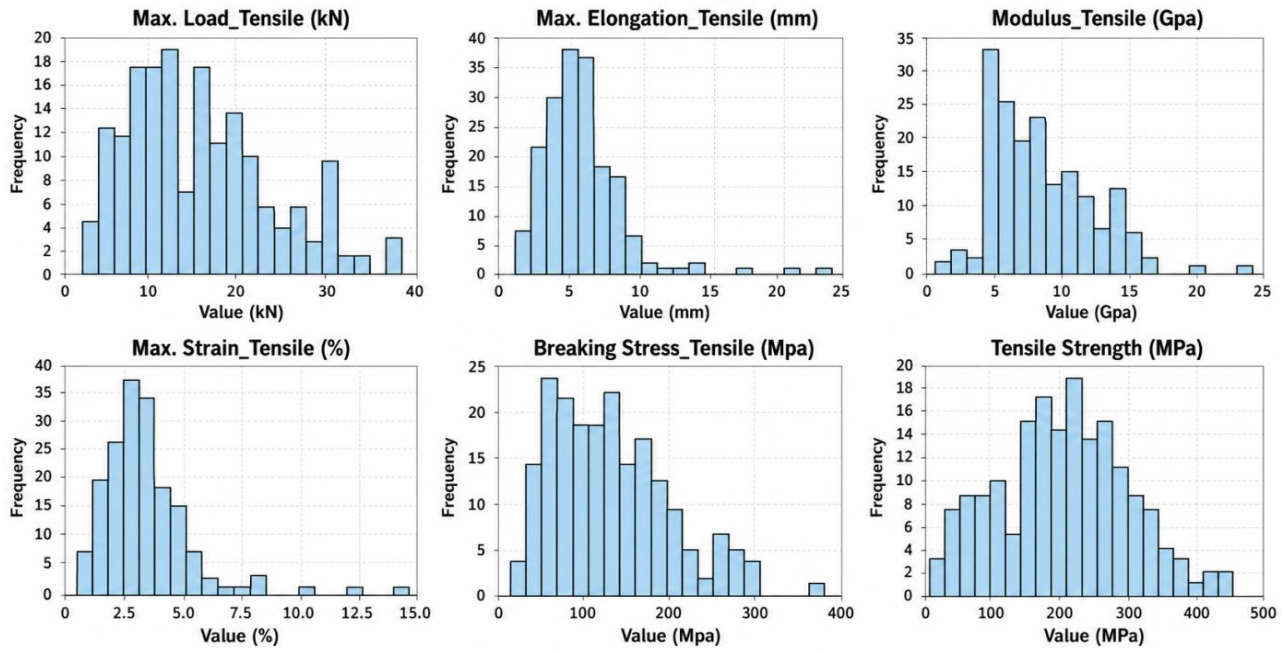


Figure 6. Data distribution of tensile properties as target features

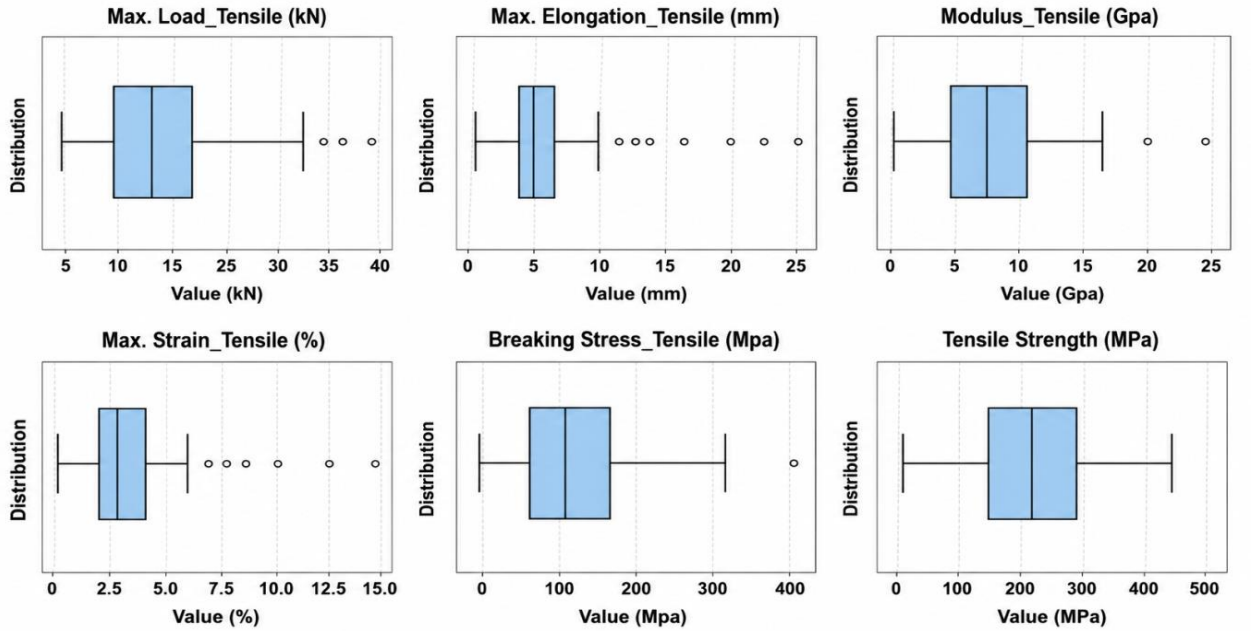


Figure 7. Boxplot of outliers of tensile properties as target features

The heat map in Figure 9 provides a holistic overview of the correlation coefficients between different parameters, revealing both expected and unexpected relationships. The strongest positive correlations were observed between the structural and thickness-related variables. For example, Calculated Thickness (mm) and Actual Thickness (mm) had an almost perfect correlation of 0.96, indicating that the calculated thickness closely matched the experimental measurements. Similarly, the number of plies had a strong positive correlation with both Calculated Thickness (mm) (0.89) and Actual Thickness (mm) (0.92), where an increase in the number of plies is directly related to an increase in material thickness. Cloth weight and thickness per ply also had a perfect correlation ($r = 1$) due to the intrinsic physical relationship between the two variables, which was kept in order to preserve material interpretability. Meanwhile, there were no adverse effects on model performance with the use of multi-collinearity robust ensemble learning methods. However, they both had negligible correlations with most mechanical performance metrics, such as Maximum Load (kN) 0.17 and Tensile Strength (MPa) 0.084. Mechanical properties had more complex relationships with each other. Max Load (kN) showed moderate positive correlations with Tensile Strength (MPa) of 0.52 and Actual Thickness (mm) of 0.51, suggesting that specimens with greater thickness or thicker specimens and higher tensile strength had greater load-bearing capacity.

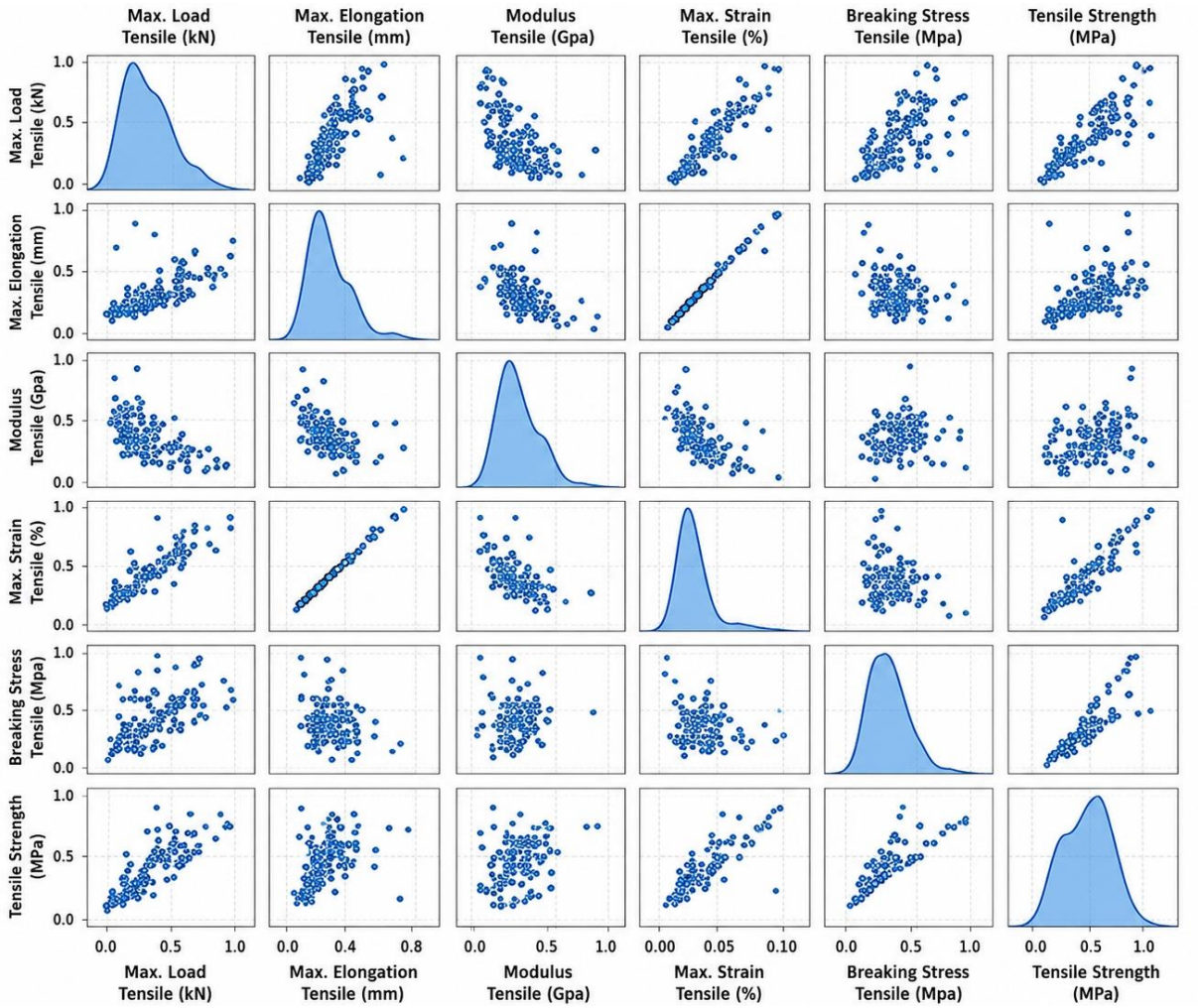


Figure 8. Pair plots of scaled tensile properties as target features

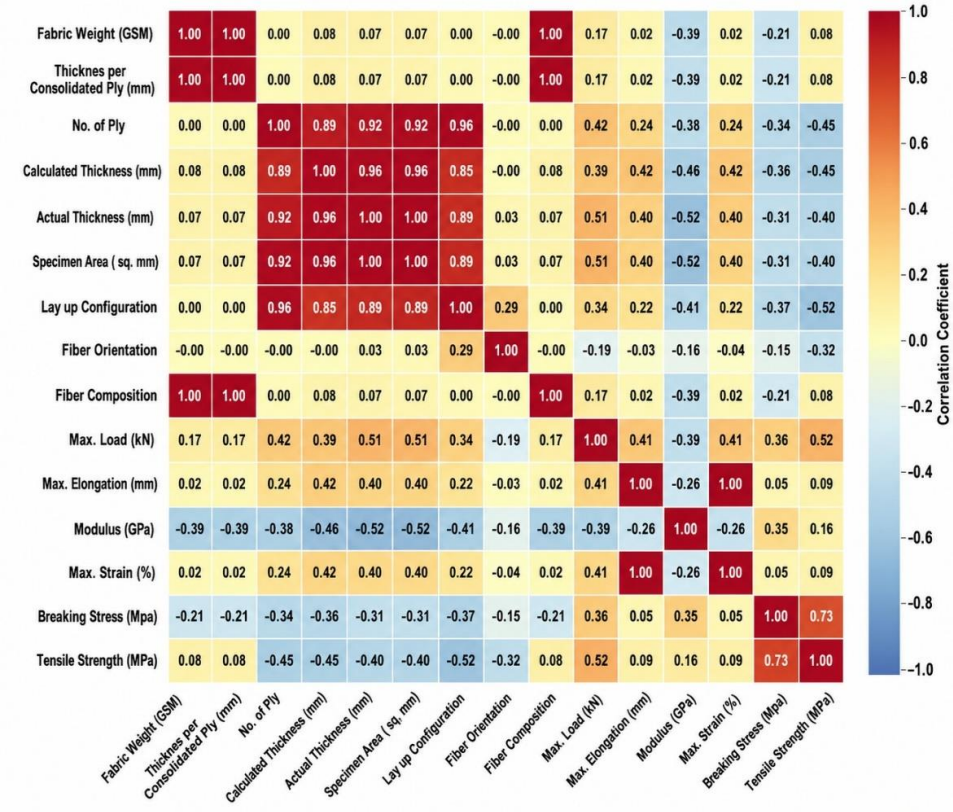


Figure 9. Correlation matrix of tensile properties as target features

Conversely, Modulus (GPa) showed weak to moderate negative correlations with the majority of variables, including Actual Thickness (mm) (-0.52), which could indicate softening of the material or nonlinear behavior under stress. Meanwhile, Breaking Stress (MPa) had a weak correlation with structural variables like Calculated Thickness (mm) (-0.36), suggesting possible trade-offs between thickness and fracture resistance. These results demonstrate the importance of feature selection in predictive modeling because variables like fiber orientation (0.034) may contribute less to explaining mechanical performance, while different fiber orientations/lay-up types determine the mechanical properties [40].

3.5.3 Analysis of feature importance

Feature importance is the average value for all target predictors and was measured using the mean decrease in R^2. It entails implementing the permutation importance of the random forest model of tensile properties. As shown in Figure 10, the model identified different dominant predictors of tensile properties, suggesting differences in the predictive variables. Tensile properties were strongly influenced by thickness (actual and calculated) as the most dominant features. It is worth noting that the number of plies and actual thickness are interdependent. Notably, the lay-up configuration also served as a significant contributor. The opposite was true for fiber orientation, which showed a moderate impact, but the number of plies and fiber composition had a negligible impact. These findings contribute to the models for the reverse thickness association. Variance in the importance of features in predicting tensile properties highlights the necessity for condition-specific approaches in modeling for composite performance prediction.

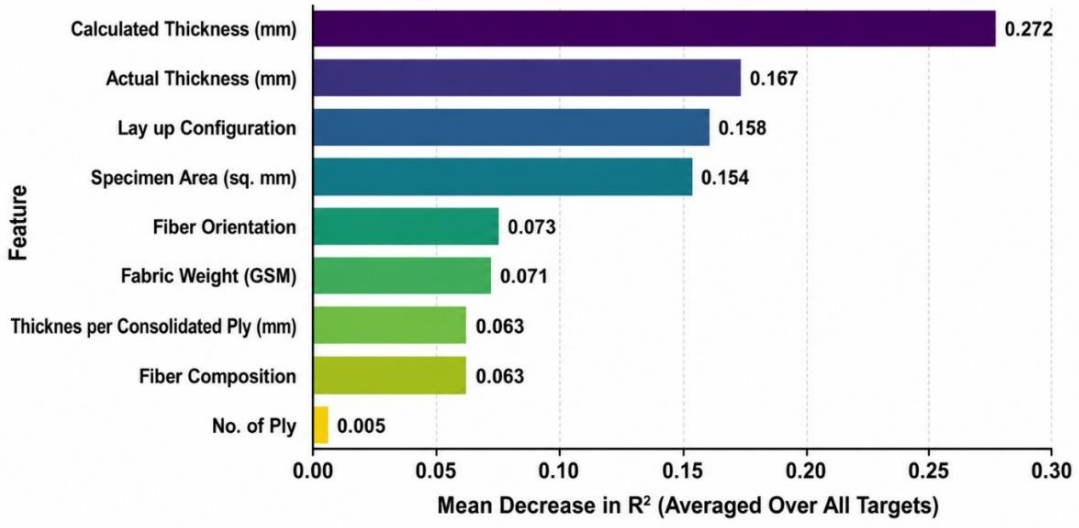


Figure 10. Feature importance of tensile properties as target features

3.5.4 Data augmentation and splitting method

This study systematically augmented the data by increasing the original dataset of 162 observations to 486 synthetic samples by injecting Gaussian noise. This technique introduced artificial variation to each feature, and the magnitude of the noise was calibrated to 1% of the standard deviation (s = 0.01 x STD) of the parameters in the respective ply. Such an augmentation was performed to maintain the original distribution characteristics of several critical deterministic values of the tensile properties (tensile strength [original STD = 81.1 MPa]; modulus [original STD = 39.05 GPa]). The augmented dataset was then divided according to an 80-20 stratified splitting protocol to ensure that it contained 518 training samples (80%) and 130 test samples (20%) with a random state of 42. Stratification was implemented based on the quintiles of important predictor variables to ensure that all material performance ranges were adequately represented in the training and validation data.

3.5.5 Models' training

A critical analysis was conducted by considering the predictive capabilities of the tested machine learning models in Table 5. Distinctive performance patterns were identified regarding the predictive capabilities of the models tested for tensile behaviors. The results showed a clear dichotomy between the tree-based ensemble models and other models, with RF, DT, Stochastic Gradient Boosting (SGB), GB, and XGBoost demonstrating the best performance on nearly the whole set of target variables. These models achieved high R^2 scores ranging from 0.90 to 0.98 and low error metrics, including MSE as low as 72.24 and MAE as low as 1.77, which were good scores given the complexity of the nonlinear relationships between input features and mechanical outputs. In contrast, LR, Support Vector Machines (SVM) with both linear and RBF kernels, and ANN had poor performance results. This was evidenced by the low R^2 values, such as 0.05 for SVM-RBF and only 0.41 for ANN with one output. Meanwhile, the high errors of MSE exceeding 1300 for ANN and LR suggest a fundamental inability to learn the underlying physical relationships governing composite behavior. This failure is predictable given the limitations of models to capture strong nonlinearity and complex interactions between features without any tuning or a more complex architecture. Both KNN and AdaBoost gave intermediate results, with the former recording respectable R^2 scores of approximately 0.85 for some of the targets. This

suggests that the instance-learning and simpler ensemble learning algorithms can give baseline experience but are eventually replaced by more sophisticated gradient boosting and bagging trees. Furthermore, the variation in performance for different target variables in Figure 11 is insightful. Properties like Max Load and Tensile Strength were not difficult for the top models to predict with a high accuracy, with R^2 greater than 0.97 for DT and XGBoost; it was difficult for the models to accurately predict Modulus and Max Elastic Strain using the trained models, with an R^2 greater than 0.81. Strain (%) was slightly tricky but highly precise for the tree-based models. This means that failure-related properties like strength and max load can be determined based on more distinctive, learnable rules in the feature space, while other properties like stiffness and deformation might be related more noisily to the input variables.

Table 5. Evaluation metrics of models' training for tensile properties as target features

Type	Model	MSE	MAE	R^2
Baseline	LR	1387.51	17.86	0.37
	SVM (Linear)	1440.71	18.01	0.33
	SVM (RBF)	1895.16	21.11	0.18
Ensemble	DT	72.24	1.77	0.96
	KNN	290.49	7.35	0.83
	RF	126.35	4.70	0.93
	AdaBoost	825.05	14.62	0.63
	GB	134.49	5.02	0.93
	XGBoost	72.24	1.78	0.96
	SGB	151.96	5.57	0.92
Neural Network	ANN	1301.85	16.71	0.41



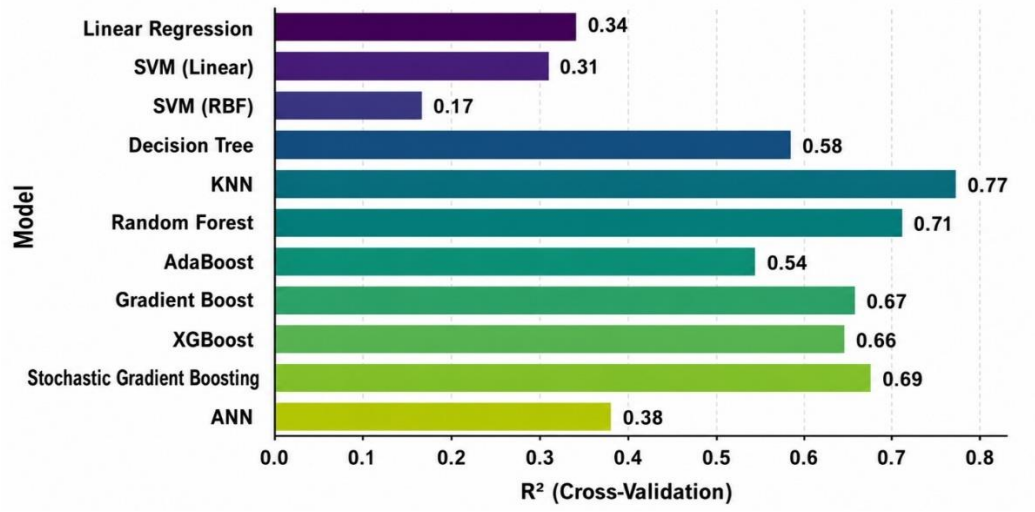
Figure 11. Heat map of models' training R^2 per target for tensile properties as target features

3.5.6 Models' validation

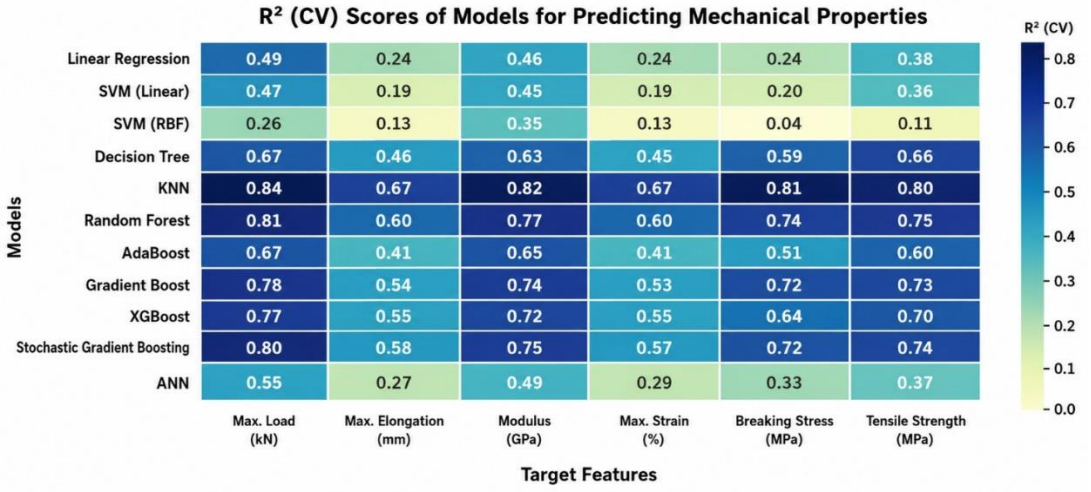
The k-fold (k = 5) cross-validation (CV) results in Figures 12(a) and 12(b) showed significant differences in the performance of various machine learning models for predicting the tensile properties of fiber-reinforced composites. The tree-based ensemble algorithms—Random Forest, Gradient Boost, Stochastic Gradient Boosting, and XGBoost—demonstrated superior performance across all evaluation measures. These models recorded the highest CV average R^2 scores between 0.67 and 0.77, reflecting a good capacity to generalize and capture the complex, nonlinear relationships present in the dataset, which could originate from the multifaceted interactions between composite constituents, parameters, and resulting mechanical behavior. The low CV Mean Squared Error and Mean Absolute Error values in Figures 13(a) and 1 (b) further confirm their reliability, accuracy, and capability in predicting key tensile properties.

In comparison, the linear models with lower complexity and the neural architecture had significantly poorer performance. Linear Regression and Support Vector Machines (both linear and RBF kernels) gave the lowest average CV R^2 values between 0.17 and 0.38 and the greatest error (MSE values exceeding 1000 in some cases). This poor performance highlights the basic deficiency of linear assumptions. This poor performance highlights the limitations of linear assumptions in modeling the highly nonlinear and complex interactions characteristic of composite material data. ANN model also underperformed compared to the tree-based ensembles (R^2 = 0.38). This suggests that without much

architecture and feature engineering, the usual ANN might struggle to efficiently learn from limited or complex datasets, while the ensemble methods using trees can perform effectively and naturally.

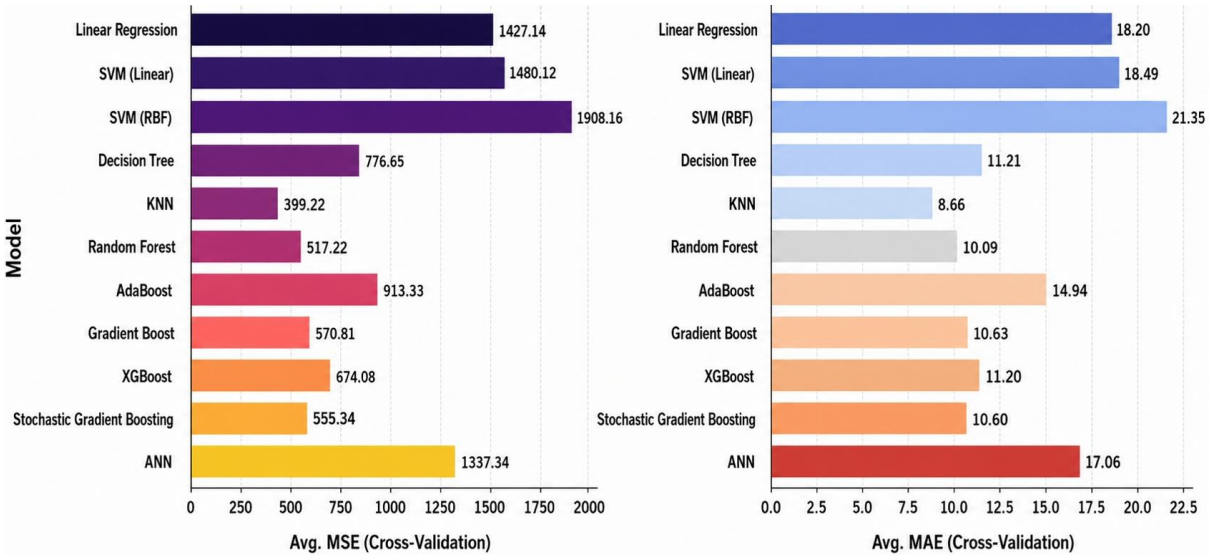


(a)



(b)

Figure 12. K-fold cross-validation: (a) R^2 per model and (b) Heat map of R^2 per target for tensile properties as target features



(a) (b)

Figure 13. K-fold cross-validation per model for tensile properties as target features: (a) MSE and (b) MAE

Interestingly, KNN demonstrated competitive and even better performance than several other models, with an average R^2 score of 0.71. This suggests that instance-based learning that exploits local similarity in feature space can make good predictions of mechanical properties for this application. However, its performance is incomparable to that of the best ensemble methods. The models' difference in efficacy for various target variables in Figure 12 (b) is equally interesting. For example, Max Load and Tensile Strength are generally predicted with higher accuracy levels, as higher R^2 across most models, compared to Max Strain (%) or Breaking Stress, suggesting that some of the mechanical properties are more intrinsically learnable from the available features than others.

3.5.7 Models' testing

The models' testing data in Table 6 assessed the performance of KNN, LR, DT, SVM-Linear, and SVM-RBF against various tensile properties. The results showed that KNN consistently performed better than other models, with a higher mean R^2 of 0.87 and R^2 values ranging between 0.83 and 0.89. The heat map of models versus target features in Figure 14 also implied the robust capabilities of GPR in predicting the tensile strength of natural fiber composites, with a correlation coefficient of 99.13% [9] and Linear Regression predictive performance of over 90% [7]. In contrast, the SVM of the RBF kernel had the weakest performance, suggesting a lack of consistency. SVM-linear performed better compared to SVM-RBF, which can be attributed to the fact that the kernel plays a role in nonlinear data. However, fundamental models generally have problems with properties, though KNN achieved the highest R^2 over all tensile properties (see Figure 15). On the other hand, ensemble models (e.g., RF, XGBoost, GB, and SGD) provided enhanced performance compared to fundamental models, except in the case of AdaBoost, with an average R^2 of 0.78 and R^2 values ranging from 0.63 to 0.84 (see Figure 16). SGB achieved high accuracy, which is close to the predictive accuracy from simulated microstructural data ($R^2 > 0.90$) of elastic modulus, shear modulus, and ultimate strengths of CFRPs [4]. Meanwhile, multiple regressor application to predict modulus, maximum stress, maximum strain, and Shore hardness revealed 63% accuracy [11], demonstrating the benefit of aggregating multiple decision trees to reduce overfitting and enhance generalizability. RF, AdaBoost, and GB also exhibited good performance. However, AdaBoost underperformed consistently and had low accuracy. This result is expected since it is based on gradient boosting, which may face issues in handling complex datasets. Overall, ensemble methods, particularly SGB, provide a balance between the robustness and accuracy of a neural network but require careful tuning to ensure that performance is maintained across all tensile properties.

Table 6. Evaluation metrics of models' testing for tensile properties as target features

Type	Model	MSE	MAE	R^2
Baseline	LR	1387.18	18.07	0.37
	SVM (Linear)	1452.49	18.45	0.30
	SVM (RBF)	1872.46	21.53	0.16
	DT	678.20	10.79	0.62
	KNN	318.84	7.73	0.87
Ensemble	RF	505.00	9.76	0.75
	AdaBoost	980.07	15.57	0.53
	GB	460.18	9.79	0.73
	XGBoost	504.36	10.08	0.73
Neural Network	SGB	446.27	9.76	0.78
	ANN	1290.14	16.75	0.41



Figure 14. Models' testing R^2 for tensile properties as target features

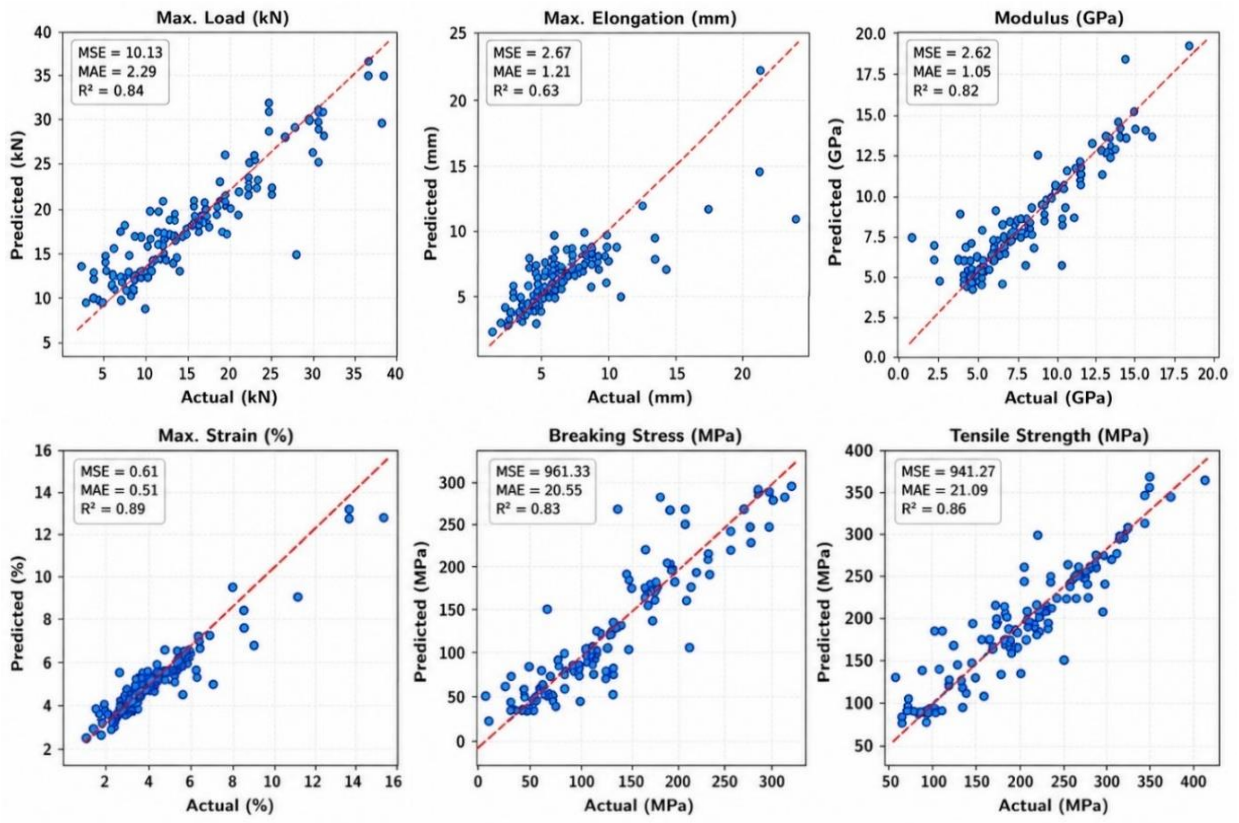


Figure 15. Actual versus predicted plot of KNN for tensile properties as target features

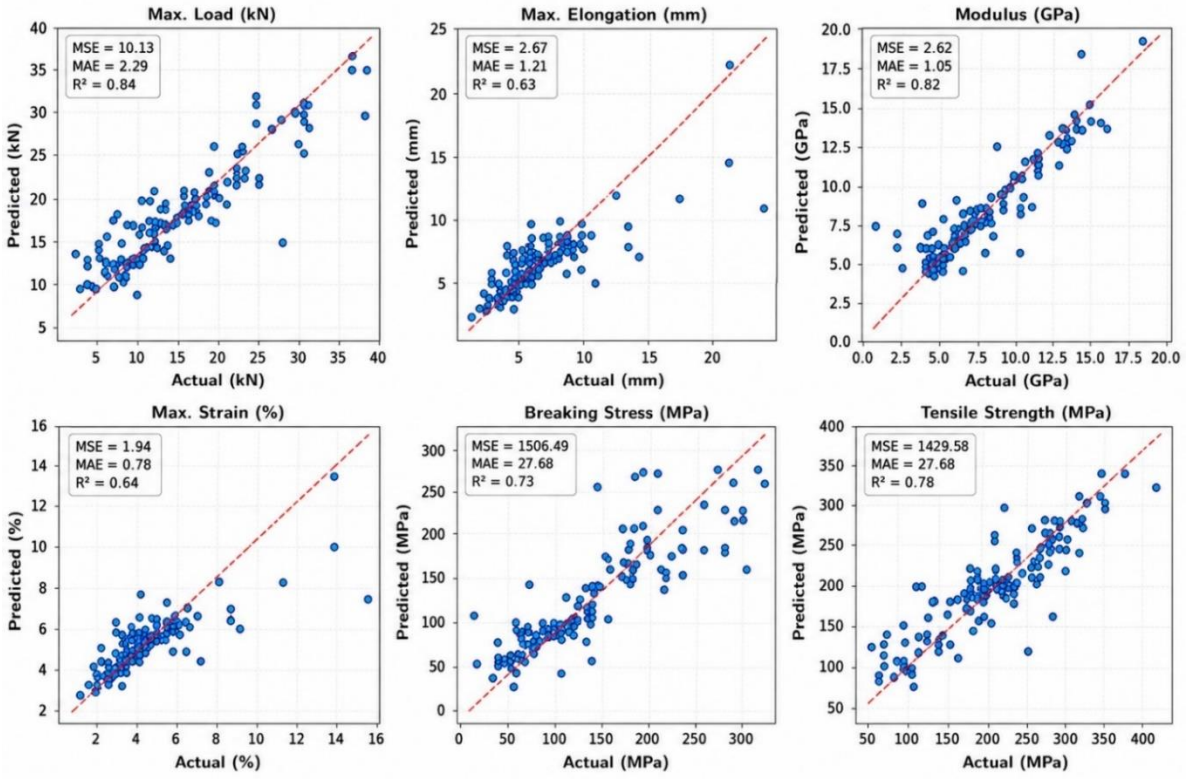


Figure 16. Actual versus predicted plot of SGB for tensile properties as target features

Figure 17 shows that the ANN model had comparatively poor performance and often matched or exceeded the linear model. Despite achieving satisfactory results for tensile properties prediction, ANN models have been successfully applied to predict the properties of eco-friendly engineered geopolymer composites [14], ultra-high performance concrete composites [17], and banana-HDPE and plantain fiber-carbon nanotube systems [18]. Nevertheless, the classification accuracy (95%) of the ANN framework comprising BPNN and SNN from the cellulose and moisture content data of natural fibers was slightly higher [20]. Regardless of the good predictive performance of both the ANN

and GPR models in the tensile and flexural properties of graphene nanoplatelet-based triaxial braided composites, the lowest RMSE value of 0.37 [28] suggests that such a performance depends on minimizing the metric for tensile properties. This dependency may stem from the representation of features or a small amount of data used. The relatively low predictive capability of ANN in predicting tensile properties was found to be inherent ($R^2 = 0.41$). Furthermore, the loading properties of mono-, bi-, and tri-fiber reinforced composites are built around the interplay of features, conditional response, and sudden changes in the properties of at least one type of fiber, in addition to the stacking sequence. These nonlinear and hierarchical relationships are difficult for feedforward ANNs to capture because of their functional processing constraints on smoothness and the requirement for large datasets to effectively learn high-order interactions. Additionally, most geometric descriptors are multicollinear, and the experimental noise is not of the heteroscedastic type, making it difficult to generalize the capability of ANNs. The overall evaluation showed that KNN is a simple and effective basic model, as evidenced by the actual and predicted plots and performance evaluation (Figure 15). Meanwhile, the ensemble technique of SGB showed robustness, as shown in Figure 16.

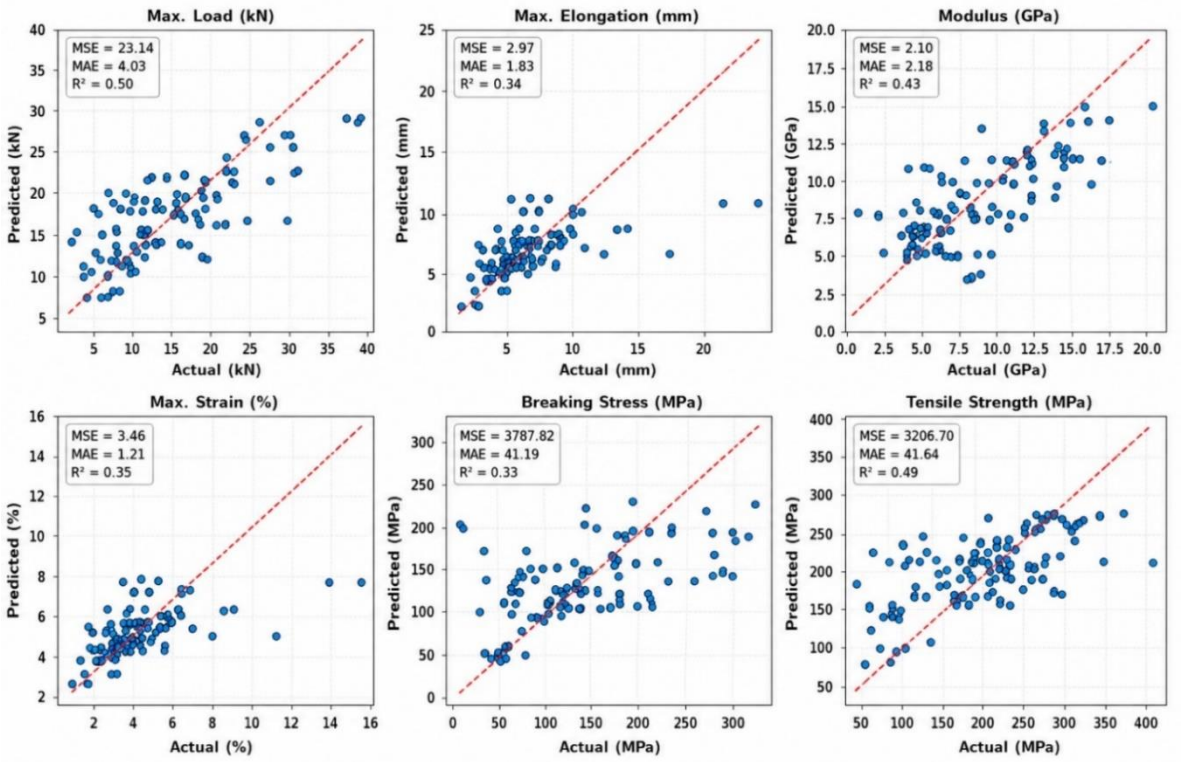


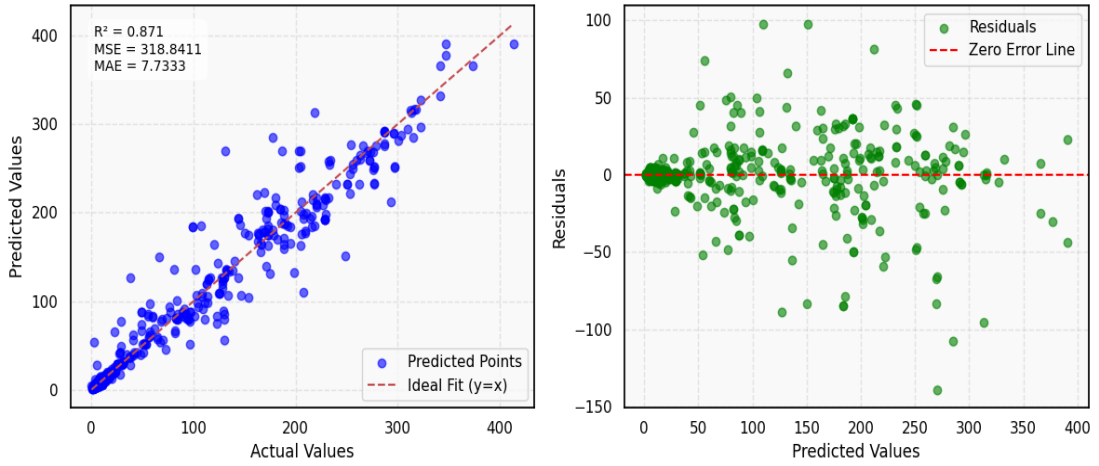
Figure 17. Actual versus predicted plot of ANN for tensile properties as target features

3.5.8 Overall performance analysis

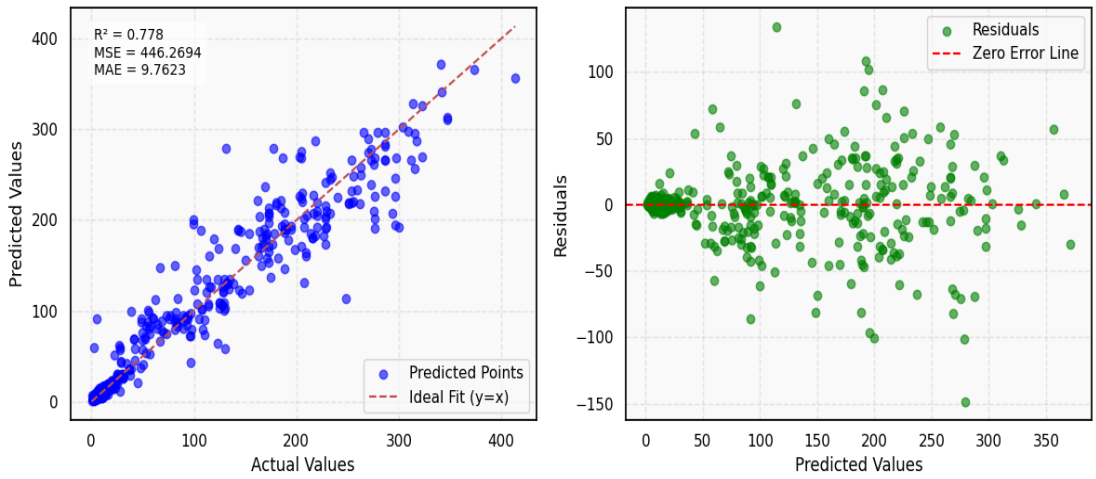
The fundamental models showed major differences in performance. KNN emerged as the most superior with the smallest Mean Squared Error, Mean Absolute Error, and an overall R^2 score of 0.87 (see Figure 18 (a)), revealing its strong predictive capability, which was 9% greater than that of the close-performing ensemble stochastic gradient boosting model. In contrast, SVM-RBF exhibited poor performance, indicating its inability to capture the underlying data trends, and hence performed worse than a horizontal line fit. Linear Regression also indicated that SVM-linear was moderately effective, and DT was in the middle.

Regarding the ensemble models, stochastic gradient boosting showed the best validation performance ($R^2 = 0.778$), as shown in the actual versus predicted and predicted versus residuals overall plots in Figure 18 (b). This indicates a better generalization performance than that of the fundamental models. Meanwhile, DT and RF showed a good correlation ($R^2 > 0.94$) for predicting the modulus of flax epoxy composites [12]. Both XGBoost and GB also performed respectably with AdaBoost. Notably, GB combined with PCA achieved approximately 5% prediction error for yield strength and stiffness prediction [46], while XGBoost Regression yielded R^2 values of 0.9714 for tensile strength prediction in composites reinforced with treated jute fibers [10] and R^2 values up to 0.993 in training and 0.957 in testing for compressive strength, tensile strength, and ductility prediction of HPFRCC [26]. These results suggest that the boosting methods were effective, although SGB achieved the best overall performance, which is further substantiated by the overall actual versus predicted and predicted versus residual plots shown in Figure 18 (b). This may be attributed to its ability to improve predictive performance through sequential boosting. Similar findings were reported by a previous study that combined ANN, SVR, RF, GBM, CNN, and RNN applications to literature and open-source data to predict tensile strength, where RF emerged as the best performer with the lowest MSE and MAE [27]. However, RNN achieved the highest R^2 value (0.98) among the Ridge Regression, RF, and MLP models, denoting RF, MLP, and RNN applications for predicting the modulus based on the carbon laminate datasets [47]. Notably, ANN

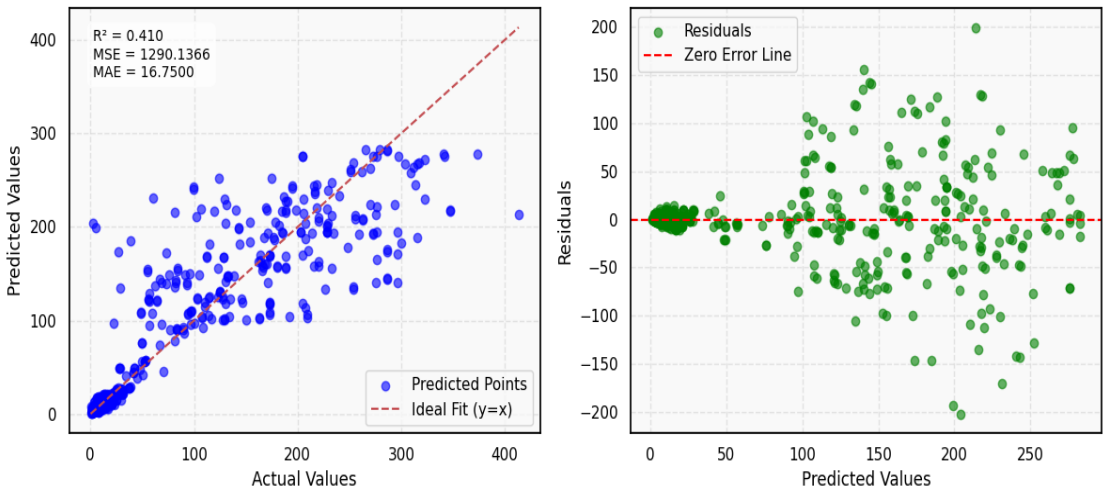
showed comparatively poor performance with the highest MSE and a lower R^2 of 0.41, as shown in the overall actual versus predicted and predicted versus residual plots in Figure 18 (c).



(a)



(b)



(c)

Figure 18. Actual versus predicted (left), predicted versus residuals (right) overall plotting: (a) KNN; (b) SGB; and (c) ANN model for tensile properties as target features

4. Conclusion

This study aimed to predict the tensile properties of composite laminates by implementing and evaluating machine learning models considering carbon fiber, Kevlar fiber, and glass fiber in pure, bi-fiber (50/50), and tri-fiber (50/25/25) compositions with varying numbers of plies (4, 8, and 12) and stacking sequences ([0°/90°/90°/0°]s and [45°/0°/-45°/90°]s). The experimental tensile tests of all 54 manufactured laminates established a performance benchmark, with

a carbon-dominated, tri-fiber, 8-ply cross-ply laminate exhibiting the highest tensile strength of 389.79 MPa. Predictive modeling was compared with a suite of ML algorithms, including baseline, ensemble, and neural network models. Analysis of the overall performance metrics revealed that K-Nearest Neighbors emerged as the best baseline estimator (R^2 = 0.87, MSE = 318.84, MAE = 7.73), whereas SGB was the high-performance ensemble model (R^2 = 0.78, MSE = 446.27, MAE = 9.76). In contrast, the ANN performed poorly (R^2 = 0.41), which can be attributed to the limitations of the available dataset. In conclusion, this study offers empirical evidence of the powerful capabilities of machine learning methods, specifically instance-based and ensemble tree methods, in addressing the complex design space of hybrid composites and predicting their tensile properties with high accuracy. However, the models were trained on a relatively small, representative experimental dataset. Therefore, future research should focus on increasing the dataset size to improve the generalizability of the findings. Critical fabrication and processing parameters can also be incorporated as input features to further improve the predictive accuracy and practical utility of the models for composite design and optimization in aerospace and automotive applications.

Acknowledgements
The Ministry of Higher Education (MoHE), Malaysia, supported this research through Universiti Tun Hussein Onn Malaysia (UTHM) under the Fundamental Research Grants Scheme.

Funding
This research was funded by the Ministry of Higher Education (MoHE) Malaysia through the Fundamental Research Grant Scheme (FRGS/1/2023/TK04/UTHM/02/1)

Declaration of Competing Interests
The authors declare no conflict of interest.

CRediT Authorship Contribution Statement
Md. Mominur Rahman: Methodology; Analysis; Investigation; Data curation; Writing-original Draft
Al Emran Ismail: Conceptualization; Analysis; Writing-review & revise; Supervision; Project Administration
Muhammad Faiz Ramli: Conceptualization; Analysis; Writing-review & revise; Supervision
Azrin Hani Abdul Rashid: Conceptualization; Analysis; Validation; Writing-review & revise; Supervision

Availability of Data and Materials
The dataset generated and analyzed during this study is available from the corresponding author upon reasonable request.

Ethics Statement
This study did not involve human participants or animal subjects. Therefore, this study did not require ethical approval.

Generative Artificial Intelligence Declarations
The authors declare that generative artificial intelligence (AI) techniques were not used to create the scientific content, concepts, analysis, or findings of this study. Any AI-assisted technologies used were for language improvement and readability enhancement, under stringent human oversight and control. The authors are responsible for the integrity, accuracy, and final content of the paper.

References
[1] E. Selver, P. Potluri, C. Soutis, and P. Hogg, "Healing potential of hybrid materials for structural composites," *Composite Structures*, vol. 122, pp. 57–66, 2015. https://doi.org/10.1016/j.compstruct.2014.11.027.
[2] A. K. Hamzat, U. T. Salman, M. S. Murad, *et al.*, "Development of robust machine learning models for predicting flexural strengths of fiber-reinforced polymeric composites," *Hybrid Advances*, vol. 8, Art. no. 100385, 2025. https://doi.org/10.1016/j.hybadv.2025.100385.
[3] R. R. Baishya and S. W. Case, "Prediction of mechanical properties of glass-epoxy composites using supervised learning," *Journal of Reinforced Plastics and Composites*, vol. 45, no. 5-6, pp. 1334-1350, 2026. https://doi.org/10.1177/07316844251318775.
[4] M. Su, L. Liu, Y. Xie, H. Peng, and C. Kang, "Prediction of the elastic properties and strength of unidirectional carbon fiber reinforced polymers based on representative volume element simulation," *Case Studies in Construction Materials*, vol. 23, Art. no. e04963, 2025. https://doi.org/10.1016/j.cscm.2025.e04963.
[5] J. K. Jatavallabhula, V. R. Veeredhi, G. S. Reddy, R. R. Baridula, and V. V. Satyanarayana, "Machine learning-based prediction of impact toughness in AISI 430–AISI 304 friction-welded joints," *International Journal of Automotive and Mechanical Engineering*, vol. 22, no. 1, pp. 12118–12132, 2025. https://doi.org/10.15282/ijame.22.1.2025.13.0930.
[6] Z. Qi, N. Zhang, Y. Liu, and W. Chen, "Prediction of mechanical properties of carbon fiber based on cross-scale FEM and machine learning," *Composite Structures*, vol. 212, pp. 199–206, 2019. https://doi.org/10.1016/j.compstruct.2019.01.042.

[7] K. Berladir, K. Antosz, V. Ivanov, and Z. Mitaľová, "Machine learning-driven prediction of composite materials properties based on experimental testing data," *Polymers*, vol. 17, no. 5, Art. no. 694, 2025. https://doi.org/10.3390/polym17050694.

[8] T. R. C. Chuaqui, A. T. Rhead, R. Butler, and C. Scarth, "A data-driven Bayesian optimisation framework for the design and stacking sequence selection of increased notched strength laminates," *Composites Part B: Engineering*, vol. 226, Art. no. 109347, 2021. https://doi.org/10.1016/j.compositesb.2021.109347.

[9] Y. Zhang and X. Xu, "Machine learning tensile strength and impact toughness of wheat straw reinforced composites," *Machine Learning with Applications*, vol. 6, Art. no. 100188, 2021. https://doi.org/10.1016/j.mlwa.2021.100188.

[10] P. Beldar and S. Kadbhane, "Utilizing machine learning to forecast mechanical characteristics of NaOH-treated jute fiber reinforced composite materials," *Materials Letters*, vol. 377, Art. no. 137411, 2024. https://doi.org/10.1016/j.matlet.2024.137411.

[11] E. Kosicka, A. Krzyzak, M. Dorobek, and M. Borowiec, "Prediction of selected mechanical properties of polymer composites with alumina modifiers," *Materials*, vol. 15, no. 3, Art. no. 882, 2022. https://doi.org/10.3390/ma15030882.

[12] T. Sadat, "Machine learning-assisted tensile modulus prediction for flax fiber/shape memory epoxy hygromorph composites," *Applied Mechanics*, vol. 4, no. 2, pp. 752–762, 2023. https://doi.org/10.3390/applmech4020038.

[13] A. Mahajan, S. Bajoliya, S. Khandelwal, *et al.*, "Comparison of ML algorithms for prediction of tensile strength of polymer matrix composites," *Materials Today: Proceedings*, vol. 116, pp. 9-14, 2022. https://doi.org/10.1016/j.matpr.2022.12.105.

[14] F. Rehman, H. Li, S. A. Khokhar, U. J. Malik, A. Hamza, and S. Song, "Development of an artificial neural network (ANN) based model for tailoring the fracture response of eco-friendly engineered geopolymer composites (EGC)," *Next Materials*, vol. 8, Art. no. 100812, 2025. https://doi.org/10.1016/j.nxmate.2025.100812.

[15] M. Li, H. Zhang, S. Li, W. Zhu, and Y. Ke, "Machine learning and materials informatics approaches for predicting transverse mechanical properties of unidirectional CFRP composites with microvoids," *Materials & Design*, vol. 224, Art. no. 111340, 2022. https://doi.org/10.1016/j.matdes.2022.111340.

[16] J. Friemann, B. Dashtbozorg, M. Fagerström, and S. M. Mirkhalaf, "A micromechanics-based recurrent neural network model for path-dependent cyclic deformation of short fiber composites," *International Journal for Numerical Methods in Engineering*, vol. 124, no. 10, pp. 2292–2314, 2023. https://doi.org/10.1002/nme.7211.

[17] A. Y. Diab and A. C. Ferche, "Prediction of tensile properties of ultra-high-performance concrete using artificial neural network," *ACI Structural Journal*, vol. 121, no. 2, pp. 57–68, 2024. https://doi.org/10.14359/51740245.

[18] J. B. anak Jores, E. Jayamani, T. S. M. Lai, J. Subramanian, and C. R. Rejeesh, "Evaluation of mechanical property of banana HDPE composite through experiment and artificial neural network (ANN)," *Materials Today: Proceedings*, vol. 103, pp. 506–512, 2024. https://doi.org/10.1016/j.matpr.2023.08.351.

[19] P. E. Imoisili, M. E. Makhatha, and T. C. Jen, "Artificial intelligence prediction and optimization of the mechanical strength of modified natural fibre/MWCNT polymer nanocomposite," *Journal of Science: Advanced Materials and Devices*, vol. 9, no. 2, Art. no. 100705, 2024. https://doi.org/10.1016/j.jsamd.2024.100705.

[20] R. Al-Jarrah and F. M. AL-Oqla, "A novel integrated BPNN/SNN artificial neural network for predicting the mechanical performance of green fibers for better composite manufacturing," *Composite Structures*, vol. 289, Art. no. 115475, 2022. https://doi.org/10.1016/j.compstruct.2022.115475.

[21] Y. Sun, I. Hanhan, M. D. Sangid, and G. Lin, "Predicting mechanical properties from microstructure images in fiber-reinforced polymers using convolutional neural networks," *Journal of Composites Science*, vol. 8, no. 10, Art. no. 387, 2024. https://doi.org/10.3390/jcs8100387.

[22] S. Sakata, G. Stefanou, Y. Arai, *et al.*, "A dual experimental/computational data-driven approach for random field modeling based strength estimation analysis of composite structures," *Computer Methods in Applied Mechanics and Engineering*, vol. 433, Art. no. 117476, 2025. https://doi.org/10.1016/j.cma.2024.117476.

[23] B. Yin, J. Huang, and W. Sun, "Peridynamics-fueled convolutional neural network for predicting mechanical constitutive behaviors of fiber reinforced composites," *Computer Methods in Applied Mechanics and Engineering*, vol. 431, Art. no. 117309, 2024. https://doi.org/10.1016/j.cma.2024.117309.

[24] J. Jung, Y. Kim, J. Park, and S. Ryu, "Transfer learning for enhancing the homogenization-theory-based prediction of elasto-plastic response of particle/short fiber-reinforced composites," *Composite Structures*, vol. 285, Art. no. 115210, 2022. https://doi.org/10.1016/j.compstruct.2022.115210.

[25] I. Malashin, V. Tynchenko, A. Gantimurov, V. Nelyub, and A. Borodulin, "A multi-objective optimization of neural networks for predicting the physical properties of textile polymer composite materials," *Polymers*, vol. 16, no. 12, Art. no. 1752, 2024. https://doi.org/10.3390/polym16121752.

[26] P. Guo, W. Meng, M. Xu, V. C. Li, and Y. Bao, "Predicting mechanical properties of high-performance fiber-reinforced cementitious composites by integrating micromechanics and machine learning," *Materials*, vol. 14, no. 12, Art. no. 3143, 2021. https://doi.org/10.3390/ma14123143.

[27] A. P. Singh, M. E. Asgar, A. K. S. Singholi, R. Rahul, and U. Gautam, "Machine learning approaches for predicting mechanical properties of composite materials," in *Proceeding of 2nd International Conference Emerging Applications of Artificial Intelligence, Machine Learning and Cybersecurity (ICAMC 2024)*, 2024, pp. 35–41. https://doi.org/10.21467/proceedings.178.5.

[28] G. V. Marrivada, P. K. Chaganti, and R. Sujith, "Experimental investigation and machine learning prediction of mechanical properties of graphene nanoplatelets based triaxial braided composites," *Materials Today Communications*, vol. 34, Art. no. 105305, 2023. https://doi.org/10.1016/j.mtcomm.2022.105305.
[29] M. Gayatri Vineela, A. Dave, and P. Kiran Chaganti, "Artificial neural network based prediction of tensile strength of hybrid composites," *Materials Today: Proceedings*, vol. 5, no. 9, pp. 19908–19915, 2018. https://doi.org/10.1016/j.matpr.2018.06.356.
[30] Q. Liu, F. Wang, W. Xiao, and J. Cui, "Binary dynamic stochastic search algorithm with support vector regression for feature selection in low-velocity impact localization problem," *Engineering Applications of Artificial Intelligence*, vol. 124, Art. no. 106554, 2023. https://doi.org/10.1016/j.engappai.2023.106554.
[31] T. Kotsiopoulos, P. Sarigiannidis, D. Ioannidis, and D. Tzovaras, "Machine learning and deep learning in smart manufacturing: The smart grid paradigm," *Computer Science Review*, vol. 40, Art. no. 100341, 2021. https://doi.org/10.1016/j.cosrev.2020.100341.
[32] D. P. Kroese, Z. I. Botev, T. Taimre, and R. Vaisman, *Data Science and Machine Learning: Mathematical and Statistical Methods*. Boca Raton, FL, USA: CRC Press, 2019. https://doi.org/10.1201/9780367816971.
[33] M. Lotz, "Mathematics of machine learning," lecture notes, Univ. of Warwick, Coventry, U.K., 2020, pp. 1–156.
[34] S. Hiremath, Y. Zhang, L. Zhang, and T. W. Kim, "Machine learning approach to evaluating impact behavior in fabric-laminated composite materials," *Results in Engineering*, vol. 23, Art. no. 102576, 2024. https://doi.org/10.1016/j.rineng.2024.102576.
[35] S. Selek and Y. Sahin, "Tensile property of carbon reinforced epoxy composites for different directions," *Eurasia Proceedings of Science, Technology, Engineering and Mathematics*, vol. 26, pp. 135–141, 2023. https://doi.org/10.55549/epstem.1409414.
[36] D. Gao, Z. Bao, W. Han, *et al.*, "Effect of strain rate on tensile properties of carbon fiber-reinforced epoxy laminates with different stacking sequences and ply orientations," *Polymers*, vol. 15, no. 12, Art. no. 2711, 2023. https://doi.org/10.3390/polym15122711.
[37] B. Nagaraj Goud, S. Sura, P. Aravind, B. Jawahar Lal, K. Sanskruti, and C. Pavan, "An experimental study on mechanical properties of Kevlar composite for aircraft structural applications," *Materials Today: Proceedings*, vol. 64, pp. 909–916, 2022. https://doi.org/10.1016/j.matpr.2022.06.053.
[38] L. R. Natarajan, S. Kathiresan, and M. Vinayagam, "Effect of fiber hybridization on bi-directionally oriented natural/glass fiber reinforced polymer composites," *Matéria (Rio de Janeiro)*, vol. 30, no. 1, Art. no. e20240648, 2025. https://doi.org/10.1590/1517-7076-RMAT-2024-0648.
[39] P. Maithil, P. Gupta, and M. L. Chandravanshi, "Study of mechanical properties of the natural-synthetic fiber reinforced polymer matrix composite," *Materials Today: Proceedings*, [vol. to be verified], pp. 1–7, 2023. https://doi.org/10.1016/j.matpr.2023.01.245.
[40] G. D. De and S. Sarkar, "Effects of fiber orientation distribution on the mechanical properties of paper," *Indian Journal of Science and Technology*, vol. 17, no. 20, pp. 2050–2055, 2024. https://doi.org/10.17485/IJST/v17i20.2536.
[41] E. D. Vial, R. J. da Silva, J. C. dos Santos, *et al.*, "Glass and aramid fibre-reinforced bio-based polymer composites manufactured by vacuum infusion: A statistical approach to their physical and mechanical properties," *Applied Composite Materials*, vol. 30, no. 5, pp. 1627–1644, 2023. https://doi.org/10.1007/s10443-023-10142-8.
[42] R. Hidayanto, D. I. Taufiq, H. Judawisastra, and R. Wirawan, "Compressive strength and elastic modulus of a 3D woven glass/polyester fire-retardant sandwich composite," *International Journal of Automotive and Mechanical Engineering*, vol. 21, no. 1, pp. 10981–10992, 2024. https://doi.org/10.15282/ijame.21.1.2024.03.0849.
[43] A. Vasudevan, R. Pandiyarajan, B. Navin Kumar, and J. Vijayarangam, "Effect of Kevlar ply orientation on mechanical characterization of Kevlar-glass fiber laminated composites," *IOP Conference Series: Materials Science and Engineering*, vol. 988, no. 1, Art. no. 012088, 2020. https://doi.org/10.1088/1757-899X/988/1/012088.
[44] K. Karthik, D. Rajamani, A. Manimaran, and J. Udayaprakash, "Evaluation of tensile properties on glass/carbon/Kevlar fiber reinforced hybrid composites," *Materials Today: Proceedings*, vol. 39, pp. 1655–1660, 2020. https://doi.org/10.1016/j.matpr.2020.06.049.
[45] A. Das Anto, S. Mia, and M. A. Hasib, "The influence of number and orientation of ply on tensile properties of hybrid composites," *Journal of Physics: Materials*, vol. 2, no. 2, Art. no. 025002, 2019. https://doi.org/10.1088/2515-7639/aaff7a.
[46] M. V. Pathan, S. A. Ponnusami, J. Pathan, *et al.*, "Predictions of the mechanical properties of unidirectional fibre composites by supervised machine learning," *Scientific Reports*, vol. 9, Art. no. 13964, 2019. https://doi.org/10.1038/s41598-019-50144-w.
[47] V. Shah, S. Zadourian, C. Yang, Z. Zhang, and G. X. Gu, "Data-driven approach for the prediction of mechanical properties of carbon fiber reinforced composites," *Materials Advances*, vol. 3, no. 19, pp. 7319–7327, 2022. https://doi.org/10.1039/d2ma00698g.